Cell wide responses to low oxygen exposure in *Desulfovibrio vulgaris* Hildenborough

Aindrila Mukhopadhyay[1,2], Alyssa M. Redding†[1,3], Marcin P. Joachimiak†[1,2], Adam P. Arkin[1,2,4], Sharon E. Borglin[1,5], Paramvir S. Dehal[1,2], Romy Chakraborty[1,5], Jil T. Geller[1,5], Terry C. Hazen[1,5], Qiang He[1,6 €], Dominique C. Joyner[1,5], Vincent J. J. Martin[1,2, ‡], Judy D. Wall[1,7], Zamin Koo Yang[1,6], Jizhong Zhou[1,6, 8], Jay D. Keasling[1,2,3,4] *

[1]Virtual Institute of Microbial Stress and Survival, [2]Physical Biosciences Division, Lawrence Berkeley National Laboratory, Berkeley, USA, [3]Department of Chemical Engineering, University of California, Berkeley, USA, [4]Department of Bioengineering, University of California, Berkeley, USA, [5]Earth Sciences Division, Lawrence Berkeley National Laboratory, Berkeley, USA, [6]Environmental Sciences Division, Oak Ridge National Laboratory, Oak Ridge, TN, USA, [7]Biochemistry and the Molecular Microbiology & Immunology Departments. University of Missouri, Columbia, USA, [8]Institute for Environmental Genomics and Department of Botany and Microbiology, Oklahoma University, Norman, OK, USA, .

*Corresponding author:

Jay D. Keasling, Berkeley Center for Synthetic Biology, 717 Potter Street, Berkeley, CA, 94720 USA, Email: keasling@berkeley.edu, Phone: 510-495-2620, Fax: 510-495-2630

† These authors contributed equally to this study.

‡Present Address: Biology Department, Centre for Structural and Functional Genomics, Concordia University, 7141 Sherbrooke West, Montreal, Quebec, Canada, H4B 1R6

€ Present Address: Department of Civil and Environmental Engineering, Temple University, Philadelphia, PA 19122

ABSTRACT

The responses of the anaerobic, sulfate-reducing *Desulfovibrio vulgaris* Hildenborough to low oxygen exposure (0.1% O_2) were monitored via transcriptomics and proteomics. Exposure to 0.1% O_2 caused a decrease in growth rate without affecting viability. A concerted up-regulation in the predicted peroxide stress response regulon (PerR) genes was observed in response to the 0.1% O_2 exposure. Several of these candidates also showed increases in protein abundance. Among the remaining small number of transcript changes was the upregulation of the predicted transmembrane tetraheme cytochrome c_3 complex. Other known oxidative stress response candidates remained unchanged during this low O_2 exposure. To fully understand the results of the 0.1% O_2 exposure, transcriptomics and proteomics data were collected for exposure to air using a similar experimental protocol. In contrast to the 0.1% O_2 exposure, air exposure was detrimental to both the growth rate and viability and caused dramatic changes at both the transcriptome and proteome levels. Interestingly, the transcripts of the predicted PerR regulon genes were down regulated during air exposure. Our results highlight the differences in the cell wide response to low and high O_2 levels of in *D. vulgaris* and suggest that while exposure to air is highly detrimental to *D. vulgaris*¸ this bacterium can successfully cope with periodic exposure to low O_2 levels in its environment.

Key words: PerR regulon, oxygen, air, stress, iTRAQ, microarray, integrated functional genomics, sulfate reducing bacteria.

INTRODUCTION

Sulfate reducing bacteria (SRB) like *Desulfovibrio spp.* are truly cosmopolitan organisms that flourish in deep subsurface sediments, rice paddies, lake and ocean sediments, insect and animal guts, sewers and oil pipelines (8, 27, 40, 41, 51). Though considered obligate anaerobes for many years after their discovery, *Desulfovibrio spp.* are found in many environments that are regularly or periodically exposed to oxygen (8, 20, 35). A number of *Desulfovibrio spp* have been documented to reduce millimolar levels of O_2 (12), and in an O_2 gradient, *Desulfovibrio vulgaris* Hildenborough localizes to very low O_2 concentrations rather than the anoxic region (30). However, *D. vulgaris* does not couple growth to O_2 respiration (8, 12), and even small amounts of O_2 affect growth adversely (57). Although *D. vulgaris* has been shown to survive long periods of air exposure (8, 9), it grows optimally in an anaerobic environment (46).

Several studies have focused on discovering the *D. vulgaris* genes involved in its oxidative stress response (7, 36), and a basic model for O_2 stress response in *D. vulgaris* has been proposed and reviewed (7, 37). *D. vulgaris* has two major mechanisms for superoxide removal, namely the superoxide reductase (Sor) and the superoxide dismutase (Sod). The Sor, also called desulfoferrodoxin or rubredoxin oxidoreductase (*rbo*), occurs as part of an operon that also encodes a rubredoxin (*rub*) and the rubredoxin oxygen oxidoreductase (*roo*). The Sor reportedly works in conjunction with peroxidases (e.g., AhpC, rubrerythrins (18, 37)) and electron transfer proteins such as rubredoxins (7) to convert superoxides to water. With regard to reactive oxygen species (ROS) removal, the Sor mechanism is considered to be the preferred pathway as it does not regenerate any intracellular O_2 (14, 26, 28, 42). The *D. vulgaris* genome encodes multiple genes, such as rubrerythrins, rubredoxins, and a nigerytherin, that are anticipated to be involved in peroxide reduction (Figure 1). The sequence analysis of the *D. vulgaris* genome (23) enabled

prediction of regulons, among which a putative PerR regulon was defined (49). The inferred PerR regulon contains the *perR* regulator and a subset of the peroxide reduction genes mentioned above (*ahpC*, *rbr*, *rbr2*, *rdl* and a conserved hypothetical protein, Figure 1). The *D. vulgaris* genome also encodes a Fe-Sod that has been shown to provide a protective mechanism in the periplasmic space where O_2-sensitive enzymes, such as the Fe-hydrogenase (HydA/B), function (17, 54). The *D. vulgaris* Sod may also work in conjunction with a catalase, an efficient enzyme that catalyzes the turnover of H_2O_2 to water and oxygen (42). Interestingly, the *D. vulgaris* catalase is encoded on a 202-kb plasmid, which has been documented to be lost during growth in ammonium-rich medium (18).

Despite these protective mechanisms, ROS, such as superoxides and peroxides, are still produced during O_2 reduction and trigger a variety of cellular damages in both aerobic and anaerobic organisms (37, 45, 53). While it is the ROS that cause the majority of O_2 related damage, O_2 itself also irreversibly deactivates critical periplasmic proteins such as reduced Fe-hydrogenases (54). Oxidative stress due to O_2 exposure is known to have multiple effects on cellular physiology, and O_2 exposure at both high and low levels can be expected to elicit cellular responses, especially for anaerobic organisms. Our current knowledge of the oxidative stress response mechanisms in *D. vulgaris* is derived mainly from studies conducted using air or 100% O_2 exposure (13, 16-18, 59). A survey of these studies also revealed that differences in experimental protocols led to important differences in cellular responses. For example, a study of oxygen responsive genes in *D. vulgaris* (18) reported a loss of viability in response to air exposure, yet a similar microarray study of air exposure (59) observed no such loss. Further, the modulation of the multiple protective mechanisms in response to low O_2 exposure was not explored. The specificity of many of these mechanisms in O_2 exposure also remains undefined,

as many of the candidate proteins are intimately linked with the redox status of the cell and may have redundant functions.

We hypothesized that a cell-wide study of *D. vulgaris* in a low oxygen environment might uncover new information about these mechanisms. Consistent with this, a recent study showed a *roo* mutant to be sensitive to 0.2% O_2 exposure (57). Cell-wide data from an air stress response may provide the perspective required to determine the specificity of responses in the low O_2 exposure. In order to minimize variability from experimental setup and to place our data in context of previous studies, we conducted controlled experiments to measure *D. vulgaris* responses to both low oxygen levels and air.

MATERIALS and METHODS

Bacterial growth and maintenance. Bacterial strains were grown and maintained as described previously (39). In brief, *Desulfovibrio vulgaris* Hildenborough (ATCC 29579) was grown in a defined lactate (60 mM)/sulfate (50 mM) medium, LS4D (39). To minimize sub-culturing during experimentation, *D. vulgaris* stocks stored at -80°C were used as a 10% (% is v/v unless otherwise indicated) inoculum into 100-200 mL of fresh LS4D medium and the cells were grown to mid-log phase (optical density at a wavelength of 600 nm (OD_{600}) of 0.3 – 0.4). For every transcriptome and proteome experiment, fresh starter cultures at mid-log phase were used as 10% inoculum into 1-3 L biomass production cultures and grown at 30°C, as noted previously (39).

Cell counts and growth assays during air and 0.1% O_2 exposure. One L of *D. vulgaris* culture in LS4D medium at mid-log phase (OD_{600} = 0.35) was sparged with either humidified, sterile N_2, 0.1% O_2 in N_2, or air (21% O_2). The sparge bottles were constructed from 2-L media

bottles with three-valve standard HPLC delivery caps (ULTRA-WARE, Kimble/Kontes). One valve was used to allow gas to enter, another for sampling, and the third for gas venting. Gas was sparged through porous Teflon tubing (International Polymer Engineering, Tempe AZ) filled with glass micro beads to keep the tubing submerged in the culture. Samples were taken at 0, 60, 120, and 240 min following exposure. For measuring growth, cells were counted using the acridine orange direct count (AODC) method (31). For measuring viability, colony forming units (CFU) were tested, for which aliquots were taken at the above time points and diluted serially in anaerobic LS4D medium to obtain 10^2 and 10^4 dilutions. A 200 μL sample of each dilution was suspended in molten LS4D containing 0.8% (w/v) agar before being spread on LS4D plates containing 1.5% (w/v) agar and grown anaerobically; colonies were counted after seven days.

Biomass production for integrated 'omics' experiments. Biomass for microarray analysis and proteomics experiments was generated as described previously (39). All production cultures were grown in triplicate. At an OD_{600} of 0.3 (initial time point, T_0), sample triplicates were collected (300 mL each for microarrays and 50 mL each for proteomics). Once T_0 sampling was completed, the stress was applied by sparging humidified, sterile air, 0.1% O_2 in N_2, air or N_2 (control) at approximately 200 mL/min through the 2 L cultures. Prior to T_0, the doubling time for *D. vulgaris* was measured to be approximately 5 hours. Samples were collected at 30, 60, 120, and 240 min after sparging was initiated. Processing and chilling times were minimized by pumping samples through a metal coil immersed in an ice bath as described previously (39). The chilled samples were harvested via centrifugation, flash frozen in liquid nitrogen, and stored at -80°C until analysis. Consistent with previous studies (18), pH measurements during sparging indicated that all treatments (N_2, 0.1% O_2, or air) resulted in a small pH (< 0.8) increase that may have been caused by H_2S and CO_2 loss during sparging. After four hours, the pH of each culture

was between 7.8 and 8.0. Using previously reported specific oxygen reducing potential of wild type *D. vulgaris* (57), it could be estimated that the maximum oxygen reducing potential of the culture is approximately 5.4 µmol O_2 / min. At a sparging rate of 200 mL /min, 7.8 µmol O_2 / min is estimated to be added to the culture (Supplementary data, Calculation S1, http://vimss.lbl.gov/Oxygen/). Measurements with Foxy Fospor-R oxygen sensor (Ocean Optics, Florida, USA) indicated that a continuous sparge with 0.1% O_2 increased the levels of dissolved O_2 in the blank media. The higher levels of O_2 (relative to the pure N_2 sparge) were detectable in a live *D. vulgaris* culture while being sparged, and ensured that there was a constant exposure to O_2 during the 0.1% O_2 treatment (Supplementary data, Figure S2, http://vimss.lbl.gov/Oxygen/).

Microarray transcriptomic experiments and data analysis. DNA microarrays using 70-mer oligonucleotide probes covering 3,482 of the 3,531 annotated protein-coding sequences of the *D. vulgaris* genome were constructed as previously described (33). Briefly, all oligonucleotides were commercially synthesized without modification by MWG Biotech Inc. (High Point, NC), prepared in 50% vol/vol DMSO (Sigma-Aldrich, St Louis, MO) and spotted onto UltraGAPS glass slides (Corning Life Sciences, Corning, NY) using a BioRobotics Microgrid II microarrayer (Genomic Solutions, Ann Arbor, MI). Each oligonucleotide probe had two replicates on a single slide. Probes were fixed onto the slides by UV cross-linking (600 mJ) according to manufacturer's protocol. Total RNA extraction, purification, and labeling were performed independently on each cell sample using previously described protocols (5). Each replicate sample consisted of cells from 300 mL cultures. Labeling of cDNA targets from purified total RNA was carried out using the reverse transcriptase reaction with random hexamer priming and the fluorophore Cy5-dUTP (Amersham Biosciences, Piscataway, NJ). Genomic

DNA was extracted from *D. vulgaris* cultures at stationary phase and labeled with the fluorophore Cy3-dUTP (Amersham Biosciences, Piscataway, NJ). To hybridize a single glass slide, the Cy5-dUTP-labeled cDNA probes obtained from stressed or unstressed cultures were mixed in equal amounts with the Cy3-dUTP-labeled genomic DNA. After washing and drying, the microarray slides were scanned using the ScanArray Express microarray analysis system (Perkin Elmer). The fluorescent intensity of both the Cy5 and Cy3 fluorophores was analyzed with ImaGene software version 6.0 (Biodiscovery, Marina Del Rey, CA).

Microarray data analyses were performed using gene models from NCBI. All mRNA changes were assessed with total genomic DNA as control. Log_2 ratios and z-scores were computed as previously described (39). A mean log_2-ratio cutoff of $\geq |2|$ across time points and an accompanying z-score $\geq |2|$ were used to identify genes whose expression changed most significantly. Searches of the microarray data with the mean gene expression profile of genes in the predicted PerR regulon were performed using the Pearson correlation coefficient as the scoring function and the Euclidean distance to sort the final search results The 0.71 correlation of the rubredoxin-like protein DVU3093, the lowest scoring gene from the predicted PerR regulon, was used as an empirical significance cutoff for the profile search results. (For additional notes and analysis information see supplementary Figure S5). All heat-maps of gene expression data were rendered as vector graphics and output in Encapsulated PostScript (EPS) format using JColorGrid (29). The rendering configuration specified a constant maximum and minimum data range (log_2 ratio range of (-6.25, 6.25)), a log_2 ratio increment of 0.5, and with the log_2 ratio color scale centered at log_2 ratio = 0.

The specificity of transcription changes in the predicted PerR regulon genes was assessed using the mean expression of genes in the regulon computed across different experimental

conditions corresponding to six previously published VIMSS studies (e.g., heat shock (5), salt stress (39), nitrite (22), and stationary phase (6)). The mean expression of genes in the PerR regulon was computed for each time point in each experiment, as well as the global mean and standard deviation across all time points and experiments. To assess the confidence of the observed gene expression changes, z-scores were computed for the mean PerR gene expression at each time point in the 0.1% O_2 and air stress experiments. Assuming a normal distribution, the 95% confidence interval corresponds to a z-score of 2, and at most 5% of the data are expected to have more significant changes. In the microaerobic experiment the z-scores were 0.4, 1.2, and 1.7 for time points 60, 120, and 240 min, respectively. In the air stress experiment, the z-scores were -0.4 -0.8, -1.3, -1.6, and -2.5, for time points 0, 10, 30, 120, and 240 min, respectively. Note that this is the only calculation of z-score across multiple experiments; all other z-scores reported in this study have been computed across the 0.1% O_2 and air exposure experiments only. Microarray data for this study is available though the URL: http://www.microbesonline.org/cgi-bin/microarray/viewExp.cgi?locusId=&expId=28+74. Raw microarray data can also be accessed through the following URLs for 0.1% O_2 exposure and air stress respectively; http://www.microbesonline.org/microarray/rawdata/exp28_E35
http://www.microbesonline.org/microarray/rawdata/exp74_E12

Proteomics and proteomics data analyses. Sample preparation, chromatography, and mass spectrometry for iTRAQ proteomics were performed as described previously (47) with modifications to the lysis buffers used. Frozen cell pellets from triplicate 50 mL cultures were thawed and pooled prior to cell lysis. For the 0.1% O_2-exposed biomass, cells were lysed via sonication in 500 mM triethylammonium bicarbonate (TEAB), pH 8.5 (Sigma-Aldrich), and the clarified lysate was used as total cellular protein. Sample denaturation, reduction, blocking,

digestion, and labeling with isobaric reagents were performed according to the manufacturer's directions (Applied Biosystems, Framingham, MA). The four-plex iTRAQ labels were used as follows: tag_{114}, T_0 control; tag_{115}, 240-minute control; tag_{116}, 240-minute 0.1% O_2 sparged; and tag_{117}, 240-minute 0.1% O_2 sparged (replicate). Tag_{116} and tag_{117} provided technical replicates to allow assessment of internal error. For the air-exposed biomass, cell pellets were lysed via sonication in lysis buffer (4 M urea, 500 mM TEAB, pH 8.5), and the clarified lysate was diluted with water to 1 M urea before being used. The same labeling procedure was used, and labels were used as follows: tag_{114}, 120-minute N_2 sparged control; tag_{115}, 240-minute N_2 sparged control; tag_{116}, 120-minute air sparged; and tag_{117}, 240-minute air sparged. Strong cation exchange (SCX) was used to separate both 0.1% O_2- and air-exposed, iTRAQ-labeled samples into 21-23 salt fractions. Fractions were desalted, dried, and separated on a C_{18} reverse phase nano-LC-MS column using a Dionex LC system coupled with an ESI-QTOF mass analyzer (QSTAR® Hybrid Quadrupole TOF, Applied Biosystems, Framingham, MA) as previously described (47).

Collected mass spectra were analyzed using Analyst 1.1 with ProQuant 1.1, ProGroup 1.0.6 (Applied Biosystems, Framingham, MA), and MASCOT version 2.1 (Matrix Science, Inc, Boston, USA). A FASTA file containing all the putative ORF sequences of *D. vuglaris*, obtained from microbesonline.org (1) was used to form the theoretical search database along with the common impurities trypsin, keratin, cytochrome *c*, and bovine serum albumin. The same search parameters were used in both programs as described previously (47). Only proteins identified by at least two unique peptides at greater than 95% confidence by both ProQuant and MASCOT were considered for further analysis.

All protein ratios were obtained from the ProQuant database using ProGroup. Tag ratios for each protein were computed as the weighted average from all peptides that were uniquely assigned to that protein. Technical replicates (tag_{116} and tag_{117} used to label 0.1% O_2 exposed biomass) were used to assess variability in quantification of Log_2 ratios. To define a cut-off for internal error, the deviation between the absolute value of $log_2(116/115)$ and $log_2(117/115)$ for a given protein was used. The internal error cut-off was set at the value of deviation at which 95% of all proteins showed deviation ≤ that value. The internal error cut-off was found to be |0.13|. To compute the level of significant change, z-score was computed for all log_2 values. Protein log_2 values with z-scores ≥ |2| were considered to be significantly changed. COG categories as defined by (52) were used to plot fraction of each COG category identified (Figure 8). Complete proteomics data can be obtained at http://vimss.lbl.gov/Oxygen/

RESULTS

Effect of different growth conditions on biomass and viability. For genome-wide assessment of cellular response, growth assays were conducted to determine the level of O_2 that affected the growth rate but was not lethal. Extended exposure to 0.05% O_2 had no overall effect on *D. vulgaris* growth (Figure 2A). Consistent with this, there were no significant changes in transcript levels under these conditions (Supplementary data, http://vimss.lbl.gov/Oxygen/). Sparging with 0.1% O_2 reduced both the growth rate and maximal growth (Figure 2A). However the cells resumed normal growth after a lag of about three growth cycles (15 hours), and colony forming units (CFU) were similar to control (Supplementary Figure S1, 3). Therefore, 0.1% O_2 was selected as the condition for the low O_2 exposure experiments in this study. Though the affect of 0.1% O_2 exposure on growth was most evident at later time points, to measure cellular

response at the transcript and protein level, biomass was collected at time points up until 240 minutes post exposure Figure 2B).

When exposed to air (21% O_2) for a similar length of time, the effect on both growth rate and viability was drastic. Direct cell counts showed that the air sparged samples contained only 40% of the number of cells present in the control (N_2 sparge) after 240 minutes of sparging. Further, a measurement of the CFU indicated that only a fraction of cells formed colonies when plated (~ 10%) compared the control culture at T_0 (Supplementary Figure S3). This result is consistent with most previous studies where a similar reduction in viability has been documented (18); there was only one exception where colony forming units remained unaffected (59).

Genome wide transcriptional response. The transcript profiles of cultures exposed to 0.1% O_2 were analyzed. Applying a $\log_2$ ratio cutoff of $\geq |2|$ in at least one time point (and $z \geq |2|$), for genes whose expression changed significantly, revealed only 12 significantly up-regulated genes. These results suggest that 0.1% O_2 exposure produced a mild perturbation in *D. vulgaris*. The up-regulated genes included five out of the six predicted members of the predicted PerR regulon (Figure 3). Few other genes with annotated functions showed a significant change; however, *tmcB* (DVU0264) and *divK* (DVU0259), were upregulated, both of which belong to an operon containing an iron sulfur cluster transmembrane ferredoxin complex. Using the same criteria, no transcript showed significant down regulation.

It is noteworthy that following an exposure to 0.1% O_2, the *perR* transcript increased with time, as did the transcripts of all other predicted PerR regulon genes (Figure 3). In addition to the predicted PerR regulon, the *D. vulgaris* genome encodes many genes thought to protect against oxidative damage that are widely present across many classes of bacteria, including superoxide dismutase (*sodB*), catalase (*kat*), and several thioredoxins (Figure 4). Based on

conservation across sulfate-reducing bacteria, several oxidative stress response genes are considered to be signature genes in SRB (5) and include predicted oxygen response candidates such as the Sor operon and several ferritins (Figure 5). Of genes encoding functions inferred to protect against oxidative damage, neither the genes widely distributed nor the signature genes showed a significant transcript change in response to 0.1% O_2 exposure. Microarray data also indicated that genes predicted to be involved in central metabolic pathways, such as the sulfate reduction pathway, ATP synthesis, and several periplasmic or cytoplasmic hydrogenases, were unaffected during 0.1% O_2 exposure (Figure 4 and 5).

In contrast, air exposure generated a large number of differentially expressed genes: 393 candidates showed a significant up-regulation whereas 454 genes were found to be down-regulated (for complete data see microarray data link provided in the methods section). Among these, genes in the predicted PerR regulon were downregulated, as were signature SRB genes and other genes considered to provide protection from oxidative stress (Figure 3, 4, 5). Further, in contrast to the response in the 0.1% O_2 exposure, significant down regulation for many genes in central pathways were recorded in air exposure (Figure 4, 5), highlighting the striking difference in *D. vulgaris* response to the two conditions. Upregulated transcripts in the air-stressed biomass included *clp* proteases, chaperone proteins, and phage shock proteins (Figure 8), suggestive of a drastic stress response. None of these genes showed any change during exposure to 0.1% O_2.

Proteomic response. An iTRAQ proteomics strategy was used to identify differences in protein content for the same samples used for microarray analysis. A total of 251 proteins were identified by two independent MS analysis software packages (see Materials and Methods and (47)). As in the microarray data, proteins were considered to be significantly changing if their

absolute z-scores exceeded two. Responses at the protein level may lag those at the transcript level and this may account for the milder proteomic changes compared to microarray results. The highest change noted was over two fold ($\log_2$ ratio = 1.37). For z-scores $\geq |2|$ there were only four proteins with increased levels and two proteins with decreased levels. Three of the six predicted PerR regulon members were identified in the proteomics data, and all were present at higher levels in the 0.1% O_2 exposed biomass (Figure 6, Table 1). Proteins for other oxygen response mechanisms, such as Sod (DVU2410), RoO (DVU3185) and members of the Sor operon were also identified but no significant changes were observed. The only other protein that showed accumulation in 0.1% O_2 exposure was a putative zinc-resistance associated protein, ZraP (DVU3384), though the mRNA levels did not reflect this change. Only two proteins, Rho (DVU1571), a predicted transcription termination factor, and IlvE (DVU3197), a predicted branched-chain amino acid aminotransferase, showed decreased levels. While many members of central metabolism (e.g., ATP synthesis, sulfate reduction, and pyruvate to acetate conversion) were identified, none of these proteins showed any significant change in response to the 0.1% O_2 exposure, consistent with microarray data.

Proteomics analysis of air-stressed biomass was conducted at both 120 min and 240 min. As can be seen in Figure 6C, the response at 120 min showed a similar trend to that at 240 min. A total of 438 proteins were identified in this analysis. Thirty-three proteins exhibited significant change after 120 min of air sparging, while sixteen changed following 240 min (Table 1). In contrast to the 0.1% O_2 exposure, in air stress, Sod (DVU2410) showed the largest increase and this increase was confirmed by immunoblotting (Supplementary Figure S4, http://vimss.lbl.gov/Oxygen/). The proteomics data from the air-stressed biomass also identified proteins in most central pathways (Table 1); however, no concerted significant changes could be

seen across any pathways. Notably, neither the ORF annotated as ZraP nor the predicted PerR regulon showed any significant change at 240mins during air exposure.

The PerR regulon expression profile. The genes of the predicted PerR regulon showed a distinct expression pattern in both the 0.1% O_2 exposure and aerobic stress across several time points (Figure 9). The mean expression profile for the predicted PerR regulon genes was used to search the remainder of the microarray data for other transcripts showing similar changes. Many transcripts correlated with the mean expression profile of the predicted PerR regulon genes across the two conditions and sets of time points. Among the genes of the predicted PerR regulon, the most correlated gene to that of the mean PerR profile was rubrerythrin (DVU3094, correlation 0.98) and the least correlated was a rubredoxin-like protein (DVU3093, 0.71). Using 0.71 as an empirical score significance cutoff, the PerR mean expression profile search identified 58 candidates. As evidence of the specificity of the information contained in the mean PerR expression profile, we analyzed the score distribution of the PerR regulon members in the search results. The top five out of six candidates from the search were five out of six members of the PerR regulon: a rubrerythrin (DVU3094) (Pearson rank/final rank 1/2, correlation 0.98), *ahpC* (2/1, 0.95), PerR (3/6, 0.94), a hypothetical protein DVU0772 (5/1, 0.89), and a putative rubrerythrin DVU2318 (6/58, 0.89) (Figure 9 and supplementary data, Figure S5 and Table S1). Six out of eight transcripts in the predicted *tmc* operon, encoding the tetraheme cytochrome c_3 complex, also showed high correlation with the PerR profile: DVU0260 (0.83), DVU0265 (0.83), DVU0267 (0.82), DVU0264 (0.80), DVU0266 (0.77), and DVU0263 (0.75). The *cydA/B* genes that encode the putative cytochrome bd oxidase were also correlated with the mean PerR regulon gene expression profile, at 0.74 and 0.69 for *cydA* and *cydB*, respectively (however, *cydB* was correlated below the level of the empirical correlation cutoff). The remaining genes in

the top matches of the profile search were ten conserved hypothetical proteins and thirty seven hypothetical proteins (Table S1, http://vimss.lbl.gov/Oxygen/).

DISCUSSION

While continuous bubbling of the *D. vulgaris* culture with 0.1% O_2 ensured cell exposure to a proportional amount of O_2, this level of O_2 exposure produced only a mild perturbation. This is reflected in the small number of genes that changed expression and the fact that no changes were observed in central metabolic genes. This may be an indication that under normal growth conditions, *D. vulgaris* already contains adequate levels of most of the enzymes required to respond to low levels of O_2 exposure. A concerted upregulation of the entire predicted PerR regulon was observed during 0.1% O_2 exposure, with *ahpC* being one of the most upregulated candidates at both the transcript and protein levels. Along with the *tmc* transmembrane cytochrome c_3 operon, these were the only cellular responses to 0.1% O_2 exposure. PerR regulons have been described in many bacteria (3, 21, 24, 25, 48, 58), and genes regulated by PerR are often involved in defense against ROS accumulation. In *D. vulgaris*, predicted members of the PerR regulon, such as a rubrerythrin (DVU0265), have been identified as important enzymes in exposure to both O_2 as well as other oxidative stresses (18).

The air stress had a much more drastic effect on a cell-wide level. The responses at the mRNA level were reproducible across biological replicates (Figure 10 B). Further, the changes in transcript levels between air stressed biomass at 120 and 240 min were self consistent, having a Pearson correlation of 0.77. The proteomics measurements for the biomass were similarly self consistent, having a Pearson correlation of 0.73 (Figure 6B). The microarray data indicated an overall down-regulation in central metabolic pathways such as sulfate reduction, ATP synthesis,

electron transfer, lactate uptake, and conversion of lactate to acetate, none of which were observed in the 0.1% O_2 exposure. The down regulation of genes such as lactate permease and lactate dehydrogenase during air exposure may be representative of cellular stress or a defensive response to prevent use of the electron donor and consequently prevent reduction of oxygen. Most importantly, upon air exposure the transcript levels for the predicted PerR regulon genes decreased overall, where transcripts for *perR* and genes encoding rubrerythrin and the putative rubrerythrin decreased consistently with time and showed 4-fold to 24-fold down regulation. These results highlight a sharp contrast in the response of *D. vulgaris* to 0.1% O_2 compared to air exposure.

Using the mean expression profile for the predicted PerR regulon genes across the two exposures, the microarray data were searched for other transcripts with similar expression profiles. The resulting list contained several members of the eight-gene operon encoding the transmembrane tetraheme cytochrome c_3 complex (DVU0258:DVU0266) and also the *cydAB* operon (DVU3270-DVU3271), encoding the cytochrome d ubiquinol oxidase proteins. The cytochrome bd oxidase system is typically involved in oxidative phosphorylation, and increases in the transcription of the corresponding genes during oxidative stress have been reported for other anaerobic bacteria, such as *D. gigas* (38), *Moorella thermoacetica* (11), and *Bacteroides fragilis* (2). These enzymes also appear to have a protective role in aerobic bacteria such as *Escherichia coli* and *Salmonella* during oxidative stress (15, 34). The existence of cytochrome bd oxidases in *D. vulgaris* has been a matter of historical discussion since pure cultures of *D. vulgaris* are unable to grow in oxygen (8). Here, the significant increase observed in transcripts for the electron transfer systems such as the *tmc* cytochrome c_3 complex and for the oxidative

phosphorylation enzymes like cytochrome bd oxidase may indicate that additional copies of these enzymes serve a protective role during the 0.1% O_2 exposure.

Several redox active proteins such as a thiol peroxidase, bacterioferritin, flavodoxin and ferredoxins also correlated with the mean PerR regulon gene expression profile. Since these candidates also increased during 0.1% O_2 exposure, they may also be required for O_2 defense in *D. vulgaris*. Other oxidative response genes, including the rubredoxin (DVU3184), present in the Sor operon, and the Sor itself, were also identified by the gene expression profile search, but no significant up-regulation of these candidates was observed. Of these fifty-eight candidates, more than one third (twenty one), have no predicted functions. Among genes for which a functional annotation exists, several chemotaxis and signal transduction genes were identified. These genes are ideal candidates for further studies to confirm any specific role in oxidative stress response.

It has been recently demonstrated that a *roo* deletion strain of *D. vulgaris* was more sensitive to microaerobic stress than the wild type (57); however, we observed no change in expression of this gene at either the transcript or protein level in the 0.1% O_2 exposure experiments. Deletion of the genes encoding Sor and Sod has been shown to create strains with greater O_2 sensitivity (18). While neither of these genes showed a significant transcriptional change during 0.1% O_2 exposure, candidates that confer fitness and ensure survival may already be present and not necessarily show changes in transcript or protein levels. Compared to the 0.1% O_2 exposure, air appears to have a severely detrimental effect on cellular growth. It should be noted however that increase in the Sod protein levels, and the few additional upregulated transcripts in oxidative stress response genes (such as putative peptide methionine sulfoxide reductases, *msrA* and *msrB* (DVU0576 and DVU1984)), in the air stressed biomass may be physiologically relevant for the small population of cells that remain viable in the air exposure.

Genes in the predicted PerR regulon have exhibited perturbations in other *D. vulgaris* functional genomics studies (e.g., heat shock (5), salt stress (39), nitrite stress (22), and stationary phase (6)). The increase in all members of this predicted regulon was also seen in heat shock (5), but the time dependent increase shown by these genes appears to be unique to the 0.1% O_2 exposure. Additionally, while a large number of upregulated genes were documented in the heat shock study, the upregulation during 0.1% O_2 exposure of the predicted PerR regulon genes constitutes a much more specific and limited transcriptional response. Taken together, it appears that PerR derepression is the primary *D. vulgaris* response to low O_2 exposure. Interestingly, the air stress transcriptomic data correlated better with that of heat shock than with the data from 0.1% O_2 exposure (Figure 10), and the predicted PerR regulated genes were significantly down regulated in air stress, further supporting the specificity of PerR derepression during low O_2 exposure. The common changes between air stress and heat shock have been also noted in a previous study (59).

Another candidate that was universally upregulated across multiple stress conditions monitored in *D. vulgaris* was a protein annotated as zinc resistance-associated protein ZraP (DVU3384). Though it was highly upregulated in both conditions studied here, DVU3384 may be a general stress response candidate. Additionally, though zinc uptake regulons have been shown to increase in O_2 exposure in *Lactobacilli* (50) and oxidative stress in *Bacillus* (19), DVU3384 may not be a zinc binding protein. In proteins with confirmed zinc binding motifs such as the *E. coli* YjaI, known to preferentially bind Zn and Ni (43), Zn binding is conferred by a two-part motif: an N-terminally located sequence, HRWHGRC, and a C-terminally located sequence, HGGHGMW. Due to the evolutionary distances between this gamma proteobacterium versus the delta sulfate reducer and the low sequence similarity to experimentally validated

proteins, more experimental proof is required to confirm the metal ion binding specificity of the *D. vulgaris* ZraP (DVU3384). However, the *D. vulgaris* ZraP sequence contains a cysteine residue in the C-terminal region as well as multiple histidine residues in the N-terminal region, both contained in glycine-rich and presumably flexible regions of the protein. Together these data suggest that the *D. vulgaris* ZraP contains a likely metal binding site and is an interesting candidate for follow up experiments.

Many bacteria traditionally categorized as anaerobic organisms, including *Helicobacter pylori* (56) and *Bacteroides fragilis* (2), contain numerous mechanisms to counter O_2 stress. Other anaerobes, such as *Clostridium spp, Moorella thermoacetica*, and *Spirillum winogradskii* (4, 10, 11, 32, 44), have also been found to tolerate transient exposure to oxic environments. While some among these are microaerophilic, *D. vulgaris*, like *H. pylori* and *Clostridium spp.*, cannot utilize O_2 for growth and is anaerobic by definition. However, our data indicate that this bacterium can survive 0.1% O_2 exposure both in terms of growth as well as cellular response and appears to be entirely suited for ecological niches that experience transient exposure to O_2. Results from previous studies have shown that the members of the Sor operon and other oxidative stress response genes are important for the survival of *D. vulgaris* in O_2 exposure (18, 55). Our study suggests that additional protection may be provided by the peroxidases in the predicted PerR regulon and membrane bound cytochromes. The very concerted increase and temporal response of the predicted PerR regulon in *D. vulgaris* upon exposure to low concentrations of oxygen is consistent with a physiological response to a condition that may be frequently encountered in the natural environment. Seasonal episodic infiltration of snow melts and rainfall events bring oxygenated waters to previously established anoxic and reducing environments. Given the ability of *D. vulgaris* to cope with low O_2 levels for short periods, these

weather related effects are unlikely to be catastrophic. Further, despite the graver consequences of exposure to higher levels of O_2, even the limited viability ensures propagation of the bacterium through this exceedingly harsh stress. This further suggests why *D. vulgaris* and other SRBs are so resilient in a variety of habitats, including those where exposure to oxygen may occur periodically.

ACKNOWLEDGEMENTS

We are grateful to Morgan Price, Eric Alm and Katherine Huang for helpful discussions. We thank Rick Huang, Richard Phan, and Mary Singer for technical help with biomass production, Barbara Giles for sharing experimental observations, and Keith Keller and Janet Jacobsen for help with the supplementary data link. This work was part Environmental Stress Pathway Project (ESPP) of the Virtual Institute for Microbial Stress and Survival (http://vimss.lbl.gov) supported by the U. S. Department of Energy, Office of Science, Office of Biological and Environmental Research, Genomics: GTL Program through contract DE-AC02-05CH11231 with LBNL. Oak Ridge National Laboratory is managed by University of Tennessee-Battelle LLC for the Department of Energy under contract DE-AC05-00OR22725.

REFERENCES

1. **Alm, E. J., K. H. Huang, M. N. Price, R. P. Koche, K. Keller, I. L. Dubchak, and A. P. Arkin.** 2005. The MicrobesOnline Web site for comparative genomics. Genome Res **15:**1015-22.
2. **Baughn, A. D., and M. H. Malamy.** 2004. The strict anaerobe *Bacteroides fragilis* grows in and benefits from nanomolar concentrations of oxygen. Nature **427:**441-4.
3. **Brenot, A., K. Y. King, and M. G. Caparon.** 2005. The PerR regulon in peroxide resistance and virulence of *Streptococcus pyogenes*. Mol Microbiol **55:**221-34.
4. **Briolat, V., and G. Reysset.** 2002. Identification of the *Clostridium perfringens* genes involved in the adaptive response to oxidative stress. J Bacteriol **184:**2333-43.
5. **Chhabra, S. R., Q. He, K. H. Huang, S. P. Gaucher, E. J. Alm, Z. He, M. Z. Hadi, T. C. Hazen, J. D. Wall, J. Zhou, A. P. Arkin, and A. K. Singh.** 2006. Global Analysis of Heat Shock Response in *Desulfovibrio vulgaris* Hildenborough. J Bacteriol **188:**1817-28.
6. **Clark, M. E., Q. He, Z. He, K. H. Huang, E. J. Alm, X. F. Wan, T. C. Hazen, A. P. Arkin, J. D. Wall, J. Z. Zhou, and M. W. Fields.** 2006. Temporal transcriptomic analysis as *Desulfovibrio vulgaris* Hildenborough transitions into stationary phase during electron donor depletion. Appl Environ Microbiol **72:**5578-88.
7. **Coulter, E. D., and D. M. Kurtz, Jr.** 2001. A role for rubredoxin in oxidative stress protection in *Desulfovibrio vulgaris*: catalytic electron transfer to rubrerythrin and two-iron superoxide reductase. Arch Biochem Biophys **394:**76-86.
8. **Cypionka, H.** 2000. Oxygen respiration by *Desulfovibrio* species. Annu Rev Microbiol **54:**827-48.
9. **Cypionka, H., F. Widdel, and N. Pfennig.** 1985. Survival of sulfate-reducing bacteria after oxygen stress, and growth in sulfate-free oxygen-sulfide gradients. FEMS Microbiol Lett **31:**39-45.
10. **Das, A., E. D. Coulter, D. M. Kurtz, Jr., and L. G. Ljungdahl.** 2001. Five-gene cluster in *Clostridium thermoaceticum* consisting of two divergent operons encoding rubredoxin oxidoreductase- rubredoxin and rubrerythrin-type A flavoprotein-high-molecular-weight rubredoxin. J Bacteriol **183:**1560-7.
11. **Das, A., R. Silaghi-Dumitrescu, L. G. Ljungdahl, and D. M. Kurtz, Jr.** 2005. Cytochrome bd oxidase, oxidative stress, and dioxygen tolerance of the strictly anaerobic bacterium *Moorella thermoacetica*. J. Bacteriol. **187:**2020-2029.
12. **Dilling, W., and H. Cypionka.** 1990. Aerobic respiration in sulfate-reducing bacteria. FEMS Microbiol Lett **71:**123-127.
13. **Dolla, A., M. Fournier, and Z. Dermoun.** 2006. Oxygen defense in sulfate-reducing bacteria. J Biotechnol **126:**87-100.
14. **Emerson, J. P., E. D. Coulter, R. S. Phillips, and D. M. Kurtz, Jr.** 2003. Kinetics of the superoxide reductase catalytic cycle. J Biol Chem **278:**39662-8.
15. **Farr, S. B., and T. Kogoma.** 1991. Oxidative stress responses in *Escherichia coli* and *Salmonella typhimurium*. Microbiol Mol Biol Rev **55:**561-585.
16. **Fournier, M., C. Aubert, Z. Dermoun, M. C. Durand, D. Moinier, and A. Dolla.** 2006. Response of the anaerobe *Desulfovibrio vulgaris* Hildenborough to oxidative conditions: proteome and transcript analysis. Biochimie **88:**85-94.

17. **Fournier, M., Z. Dermoun, M. C. Durand, and A. Dolla.** 2004. A new function of the *Desulfovibrio vulgaris* Hildenborough [Fe] hydrogenase in the protection against oxidative stress. J Biol Chem **279:**1787-93.
18. **Fournier, M., Y. Zhang, J. D. Wildschut, A. Dolla, J. K. Voordouw, D. C. Schriemer, and G. Voordouw.** 2003. Function of oxygen resistance proteins in the anaerobic, sulfate-reducing bacterium *Desulfovibrio vulgaris* Hildenborough. J Bacteriol **185:**71-9.
19. **Gaballa, A., and J. D. Helmann.** 2002. A peroxide-induced zinc uptake system plays an important role in protection against oxidative stress in *Bacillus subtilis*. Mol Microbiol **45:**997-1005.
20. **Hardy, J., Hamilton, W. A.** 1981. The oxygen tolerance of sulfate-reducing bacteria isolated from North Sea waters. Current Microbiology **6:**259-262.
21. **Hayashi, K., T. Ohsawa, K. Kobayashi, N. Ogasawara, and M. Ogura.** 2005. The H2O2 stress-responsive regulator PerR positively regulates *srfA* expression in *Bacillus subtilis*. J Bacteriol **187:**6659-67.
22. **He, Q., K. H. Huang, Z. He, E. J. Alm, M. W. Fields, T. C. Hazen, A. P. Arkin, J. D. Wall, and J. Zhou.** 2006. Energetic consequences of nitrite stress in *Desulfovibrio vulgaris* Hildenborough, inferred from global transcriptional analysis. Appl Environ Microbiol **72:**4370-81.
23. **Heidelberg, J. F., R. Seshadri, S. A. Haveman, C. L. Hemme, I. T. Paulsen, J. F. Kolonay, J. A. Eisen, N. Ward, B. Methe, L. M. Brinkac, S. C. Daugherty, R. T. Deboy, R. J. Dodson, A. S. Durkin, R. Madupu, W. C. Nelson, S. A. Sullivan, D. Fouts, D. H. Haft, J. Selengut, J. D. Peterson, T. M. Davidsen, N. Zafar, L. Zhou, D. Radune, G. Dimitrov, M. Hance, K. Tran, H. Khouri, J. Gill, T. R. Utterback, T. V. Feldblyum, J. D. Wall, G. Voordouw, and C. M. Fraser.** 2004. The genome sequence of the anaerobic, sulfate-reducing bacterium *Desulfovibrio vulgaris* Hildenborough. Nat Biotechnol **22:**554-9.
24. **Helmann, J. D., M. F. Wu, A. Gaballa, P. A. Kobel, M. M. Morshedi, P. Fawcett, and C. Paddon.** 2003. The global transcriptional response of Bacillus subtilis to peroxide stress is coordinated by three transcription factors. J Bacteriol **185:**243-53.
25. **Horsburgh, M. J., M. O. Clements, H. Crossley, E. Ingham, and S. J. Foster.** 2001. PerR controls oxidative stress resistance and iron storage proteins and is required for virulence in *Staphylococcus aureus*. Infect Immun **69:**3744-54.
26. **Imlay, J. A.** 2002. What biological purpose is served by superoxide reductase? J Biol Inorg Chem. 2002 **7:**659-63.
27. **Jayaraman, A., P. J. Hallock, R. M. Carson, C. C. Lee, F. B. Mansfeld, and T. K. Wood.** 1999. Inhibiting sulfate-reducing bacteria in biofilms on steel with antimicrobial peptides generated in situ. Appl Microbiol Biotechnol **52:**267-75.
28. **Jenney, F. E., Jr., M. F. n. J. n. M. Verhagen, X. Cui, and M. W. n. W. Adams.** 1999. Anaerobic microbes: oxygen detoxification without superoxide dismutase. Science **286:**306-309.
29. **Joachimiak, M. P., J. L. Weisman, and B. May.** 2006. JColorGrid: software for the visualization of biological measurements. BMC Bioinformatics **7:**225.
30. **Johnson, M. S., I. B. Zhulin, M. E. Gapuzan, and B. L. Taylor.** 1997. Oxygen-dependent growth of the obligate anaerobe *Desulfovibrio vulgaris* Hildenborough. J Bacteriol **179:**5598-601.

31. **Kepner, R. L., Jr., and J. R. Pratt.** 1994. Use of fluorochromes for direct enumeration of total bacteria in environmental samples: past and present. Microbiol Rev **58:**603-15.
32. **Lehmann, Y., L. Meile, and M. Teuber.** 1996. Rubrerythrin from *Clostridium perfringens*: cloning of the gene, purification of the protein, and characterization of its superoxide dismutase function. J Bacteriol **178:**7152-8.
33. **Li, X., Z. He, and J. Zhou.** 2005. Selection of optimal oligonucleotide probes for microarrays using multiple criteria, global alignment and parameter estimation. Nucleic Acids Res **33:**6114-23.
34. **Lindqvist, A., J. Membrillo-Hernandez, R. K. Poole, and G. M. Cook.** 2000. Roles of respiratory oxidases in protecting *Escherichia coli* K12 from oxidative stress. Antonie Van Leeuwenhoek **78:**23-31.
35. **Lobo, Melo, Carita, Teixeira, and Saraiva.** 2007. The anaerobe *Desulfovibrio desulfuricans* ATCC 27774 grows at nearly atmospheric oxygen levels. FEBS Lett **581:**433-436.
36. **Lumppio, H. L., N. V. Shenvi, R. P. Garg, A. O. Summers, and D. M. Kurtz, Jr.** 1997. A rubrerythrin operon and nigerythrin gene in *Desulfovibrio vulgaris* (Hildenborough). J Bacteriol **179:**4607-15.
37. **Lumppio, H. L., N. V. Shenvi, A. O. Summers, G. Voordouw, and D. M. Kurtz, Jr.** 2001. Rubrerythrin and rubredoxin oxidoreductase in *Desulfovibrio vulgaris*: a novel oxidative stress protection system. J Bacteriol **183:**101-8.
38. **Machado, P., R. Felix, R. Rodrigues, S. Oliveira, and C. Rodrigues-Pousada.** 2006. Characterization and expression analysis of the cytochrome bd oxidase operon from *Desulfovibrio gigas*. Curr Microbiol **V52:**274-281.
39. **Mukhopadhyay, A., Z. He, E. J. Alm, A. P. Arkin, E. E. Baidoo, S. C. Borglin, W. Chen, T. C. Hazen, Q. He, H.-Y. Holman, K. Huang, R. Huang, D. C. Joyner, N. Katz, M. Keller, P. Oeller, A. Redding, J. Sun, J. Wall, J. Wei, Z. Yang, H.-C. Yen, J. Zhou, and J. D. Keasling.** 2006. Salt stress in *Desulfovibrio vulgaris* Hildenborough: an integrated genomics approach. J. Bacteriol. **188:**4068-4078.
40. **Nemati, M., G. E. Jenneman, and G. Voordouw.** 2001. Mechanistic study of microbial control of hydrogen sulfide production in oil reservoirs. Biotechnol Bioeng **74:**424-34.
41. **Neria-Gonzalez, I., E. T. Wang, F. Ramirez, J. M. Romero, and C. Hernandez-Rodriguez.** 2006. Characterization of bacterial community associated to biofilms of corroded oil pipelines from the southeast of Mexico. Anaerobe **12:**122-33.
42. **Niviere, V., and M. Fontecave.** 2004. Discovery of superoxide reductase: an historical perspective. J Biol Inorg Chem **9:**119-23.
43. **Noll, M., K. Petrukhin, and S. Lutsenko.** 1998. Identification of a novel transcription regulator from *Proteus mirabilis*, PMTR, revealed a possible role of YJAI protein in balancing zinc in *Escherichia coli*. J Biol Chem **273:**21393-21401.
44. **Podkopaeva, D. A., M. Grabovich, and G. A. Dubinina.** 2003. Oxidative stress and antioxidant cell protection systems in the microaerophilic bacterium *Spirillum winogradskii*. Mikrobiologiia **72:**600-8.
45. **Poole, R. K.** 1994. Oxygen reactions with bacterial oxidases and globins: binding, reduction and regulation. Antonie Van Leeuwenhoek **65:**289-310.
46. **Postgate, J. R.** 1984. The Sulfate-Reducing Bacteria. Cambridge University Press, Cambridge.

47. **Redding, A. M., A. Mukhopadhyay, D. C. Joyner, T. C. Hazen, and J. D. Keasling.** 2006. Study of nitrate stress in *Desulfovibrio vulgaris* Hildenborough using iTRAQ proteomics. Brief Funct Genomic Proteomic **5:**133-143.
48. **Ricci, S., R. Janulczyk, and L. Bjorck.** 2002. The regulator PerR is involved in oxidative stress response and iron homeostasis and is necessary for full virulence of *Streptococcus pyogenes*. Infect Immun **70:**4968-76.
49. **Rodionov, D. A., I. Dubchak, A. Arkin, E. Alm, and M. S. Gelfand.** 2004. Reconstruction of regulatory and metabolic pathways in metal-reducing delta-proteobacteria. Genome Biol **5:**R90.
50. **Scott, C., H. Rawsthorne, M. Upadhyay, C. A. Shearman, M. J. Gasson, J. R. Guest, and J. Green.** 2000. Zinc uptake, oxidative stress and the FNR-like proteins of *Lactococcus lactis*. FEMS Microbiol Lett **192:**85-9.
51. **Tanaka, Y., M. Sogabe, K. Okumura, and R. Kurane.** 2002. A highly selective direct method of detecting sulphate-reducing bacteria in crude oil. Lett Appl Microbiol **35:**242-6.
52. **Tatusov, R. L., E. V. Koonin, and D. J. Lipman.** 1997. A genomic perspective on protein families. Science **278:**631-7.
53. **Valentine JS, W. D., Lyons TJ, Liou LL, Goto JJ, Gralla EB.** 1998. The dark side of dioxygen biochemistry. Curr Opin Chem Biol. **2:**253-62.
54. **Vincent, K. A., A. Parkin, O. Lenz, S. P. J. Albracht, J. C. Fontecilla-Camps, R. Cammack, B. Friedrich, and F. A. Armstrong.** 2005. Electrochemical definitions of O_2 sensitivity and oxidative inactivation in hydrogenases. J. Am. Chem. Soc. **127:**18179-18189.
55. **Voordouw, J. K., and G. Voordouw.** 1998. Deletion of the rbo gene increases the oxygen sensitivity of the sulfate-reducing bacterium *Desulfovibrio vulgaris* Hildenborough. Appl Environ Microbiol **64:**2882-7.
56. **Wang, G., P. Alamuri, and R. J. Maier.** 2006. The diverse antioxidant systems of *Helicobacter pylori*. Mol Microbiol **61:**847-860.
57. **Wildschut, J. D., R. M. Lang, J. K. Voordouw, and G. Voordouw.** 2006. Rubredoxin:oxygen oxidoreductase enhances survival of *Desulfovibrio vulgaris* Hildenborough under microaerophilic conditions. J. Bacteriol. **188:**6253-6260.
58. **Wu, H. J., K. L. Seib, Y. N. Srikhanta, S. P. Kidd, J. L. Edwards, T. L. Maguire, S. M. Grimmond, M. A. Apicella, A. G. McEwan, and M. P. Jennings.** 2006. PerR controls Mn-dependent resistance to oxidative stress in *Neisseria gonorrhoeae*. Mol Microbiol **60:**401-16.
59. **Zhang, W., D. E. Culley, M. Hogan, L. Vitiritti, and F. J. Brockman.** 2006. Oxidative stress and heat-shock responses in *Desulfovibrio vulgaris* by genome-wide transcriptomic analysis. Antonie Van Leeuwenhoek **90:**41-55.

Figure Captions

Figure 1. Overview of selected O_2 responsive proteins in *D. vulgaris*. (A) Localization and mechanistic role of individual proteins in O_2 reduction in the Gram negative *D. vulgaris* cell are shown. While all candidates are represented in the transcriptome data, those for which proteomics data was available are colored grey. Also shown is the Fenton's reaction between Fe^{2+} and H_2O_2 which generates harmful hydroxyl radicals. (B) The predicted PerR regulon (candidates with potential PerR binding motifs) and other selected candidates. Underlined genes are reported to encode NADH peroxidases. DVU numbers are shown in parentheses.

Figure 2. Effect of O_2 exposure on growth of *D. vulgaris.* Growth of *D. vulgaris* was measured via cell count / ml (AODC). Each measurement is an average of three technical replicates. **(A)** *D. vulgaris* cell counts after sparging (200 ml/min) with 0.05% O_2 in N_2 (open triangle), 0.1 % O_2 in N_2 (filled square), or N_2 (open square) measured over 60 hours. Over the 72 hour period, *D. vulgaris* showed similar growth profiles in 0.5% O_2 and N_2 (control), while in 0.1% O_2 a much lower maximal growth was observed. **(B)** *D. vulgaris* cell count after sparging (200 ml/min) with N_2 (open bar) compared to 0.1% O_2 (filled bar) at 0 and 240 minutes. In order to assess the cell wide changes initiated in response to the 0.1% O_2 exposure, biomass for transcript and protein analysis was collected at 240 min after initiation of exposure, prior to entering stationary phase. Note that the effect of 0.1% O_2 sparge is only evident at later time points.

Figure 3. Genes whose expression changed most significantly in response to 0.1% O_2 exposure (cut-off threshold of $\log_2 R \geq 2$ and corresponding $Z \geq 2$). Heat map shows changes in mRNA

levels over time (in minutes) in response to either 0.1% O_2 or air stress. The range of changes observed for these two experiments are shown in the key as $\log_2$ R adjacent to the heat map. * Predicted PerR regulon genes.

Figure 4. Transcriptomic response of selected genes in 0.1% O_2 and air exposed cultures. The heat map shows changes in mRNA levels over time (in minutes) in response to either 0.1% O_2 or air stress. Candidates are grouped by function or gene ID numbers and are not from an automated clustering. The range of changes observed for these two experiments are shown in the key adjacent to the heat map. Included candidates are genes considered important in redox changes, and genes for central pathways such as electron transport, ATP synthesis, carbon uptake and metabolism.

Figure 5. Transcriptomic response of signature SRB genes during 0.1% O_2 and air exposure. The heat map shows changes in mRNA levels over time in response to either 0.1% O_2 or air stress. Signature genes as described in Chhabra et al 2006 were used. Genes have been categorized by function. The range of changes observed for these two experiments are shown in the key adjacent to the heat map.

Figure 6. iTRAQ proteomics for exposure to 0.1% O_2 and air. **(A)** The 0.1% O_2-exposed sample was labeled with both tag_{116} (replicate 1) and tag_{117} (replicate 2), allowing the assessment of the internal error. **(B)** The plots shows $\log_2$ (0.1% O_2/T0) vs. $\log_2$ (N_2/T0). Proteins whose z-score $\geq$ |2| were considered significant, and these candidates are highlighted as shown in the legend. **(C)** Log_2(air/N_2) at 120 minutes compared to the $\log_2$(air/N_2) at 240 minutes. Proteins

that have the same level of change in both time points would fall on the 45° line. Clustering of data around the 45° line demonstrated that there is a trend in changes observed between 120 minutes and 240 minutes. Selected proteins are color-coded as described in the legend.

Figure 7. Protein distribution in clusters of orthologous groups (COGs). Proteins identified in the proteomics data cover all major COG categories (except B and V, having 1 and 32 proteins, respectively). In each COG category, fraction of protein that showed an increase and decrease in the air stress is shown in hashed bars and filled bars respectively. The grey bar bars indicate the fraction of proteins identified and the bars with horizontal lines indicates fraction of the total predicted proteome belonging to that category. The COG categories are sorted in order of decreasing fraction identified (grey bar). Notably, the highest fraction of changes was observed in COG category S (function unknown). COGs R, L, U, and T appear under-represented. Category U contains many membrane proteins, which are often not present in high abundance. The low abundance of signaling proteins may also be the reason for disproportionately low identification of proteins in COG T. The label X represents all proteins with no assigned COG and is the largest fraction of the total proteome, containing 1066 proteins.

Figure 8. Comparison between proteomics and microarray data for selected candidates. This is a graphical representation of data presented in Table 1. Open symbols represent 0.1% O_2 exposure, whereas the solid symbols represent air exposure. Circle 1 highlights all of the candidates belonging to the low oxygen exposure. The most significant changes occurred in oxidative stress genes and in ZraP. Air exposure caused a much larger level of change. Circle 2 highlights the large increases observed in proteases and chaperones during air exposure. Circle 3

highlights the group of periplasmic binding ABC transport proteins that show an opposite trend, namely increased protein levels but decreased transcript levels. More candidates show this trend, compared to the few candidates that show increased transcript levels but decreased protein levels (top left hand quadrant).

Figure 9. Analysis of microarray data to extract genes that show changes correlated with changes in the predicted PerR regulon. **(A)** Heat map shows changes in mRNA levels for the predicted members of the PerR regulon in 0.1% O_2 and air exposure. Average trend for each time point over all the members is shown in the bottom panel. The average values from (A) were used to search the entire data set. A Pearson correlation similarity measure showed 58 genes with a trend better than or equal to the worst fitting member of the PerR regulon (Supplementary Figure S4). **(B)** Heat map for mRNA changes for these 58 genes. Color legend indicates the predicted functional category of these genes. For complete details of this list, see Supplementary Table T1.

Figure 10. Microarray data for air stress. **(A)** Comparison of mRNA data for exposure to 0.1% O_2 vs. exposure air shows no linear relationship, (Pearson correlation coefficient = 0.03, p-value = 0.01805). **(B)** Comparison mRNA data of two biological replicates of air exposure at 240 min. Though exposure to air created a heterogeneous population, the responses from two different biological replicates correlate strongly (Pearson correlation coefficient value of 0.69, p-value < 0.000005). Note that data for the second biological replicate is from an independent experiment. **(C)** Heat shock (50ºC, 120 min) data from (5) was compared with the 120 min air exposure data. Direct comparisons of these data were possible because both experiments used the same

1 microarray design, the biomass samples came from the same pipeline, and the microarray
2 experiments used genomic DNA as control. A stronger linear relationship exists between the
3 overall trends observed for heat shock vs. air exposure (Pearson correlation coefficient value of
4 0.45, p-value < 0.000005). All p values are one-tailed t-statistic based.
5

A

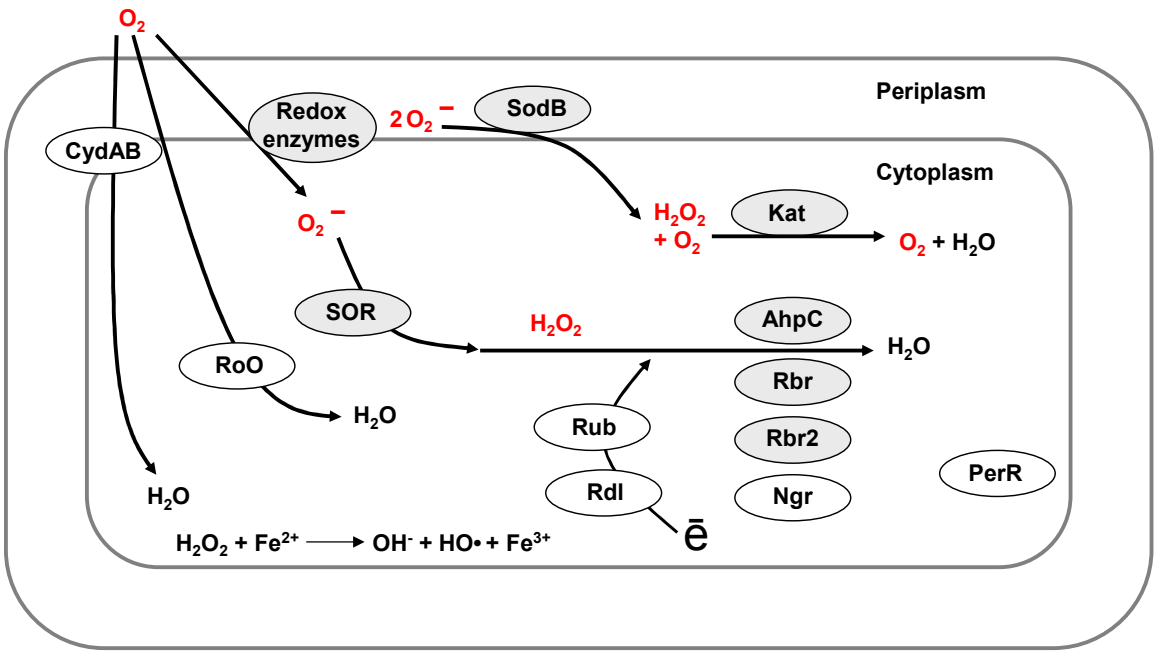
O2
Periplasm
Redox enzymes
2 O2 −
SodB
CydAB
Cytoplasm
O2 −
H2O2 + O2
Kat
O2 + H2O
SOR
H2O2
AhpC
H2O
RoO
Rbr
H2O
Rub
Rbr2
PerR
Rdl
Ngr
H2O
H2O2 + Fe2+ → OH- + HO• + Fe3+
ē

B

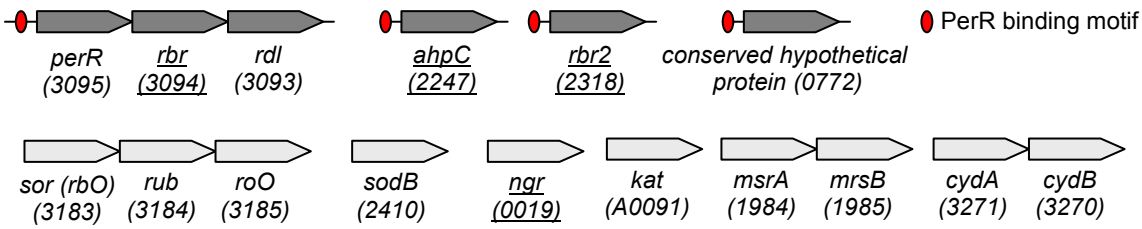
PerR binding motif
perR (3095)
rbr (3094)
rdl (3093)
ahpC (2247)
rbr2 (2318)
conserved hypothetical protein (0772)
sor (rbO) (3183)
rub (3184)
roO (3185)
sodB (2410)
ngr (0019)
kat (A0091)
msrA (1984)
mrsB (1985)
cydA (3271)
cydB (3270)

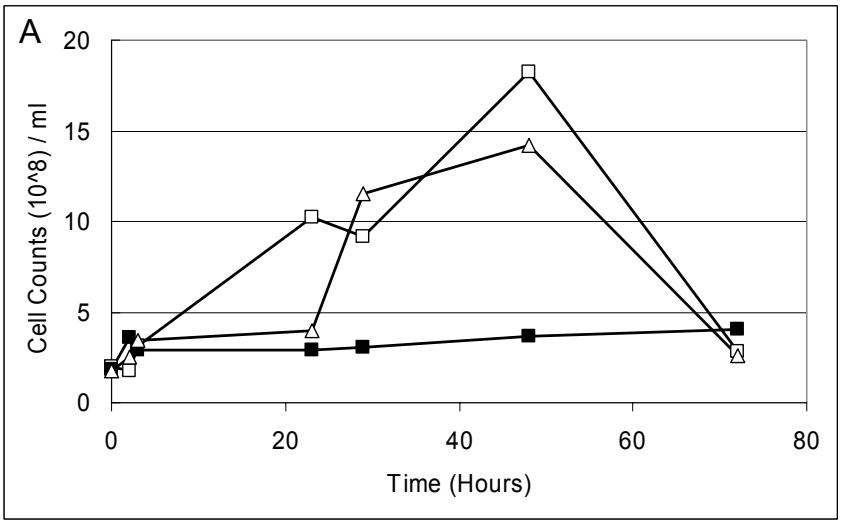
A
20
15
10
5
0
Cell Counts (10^8) / ml
0
20
40
60
80
Time (Hours)

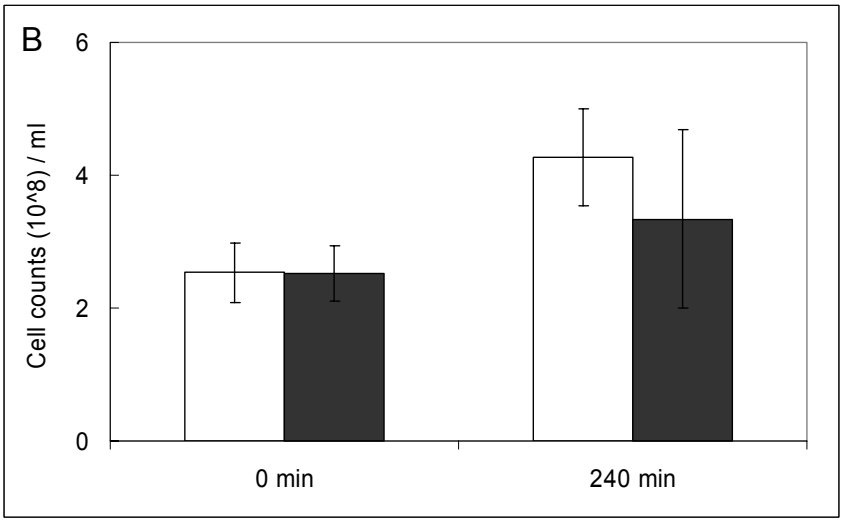
B
6
4
2
0
Cell counts (10^8) / ml
0 min
240 min

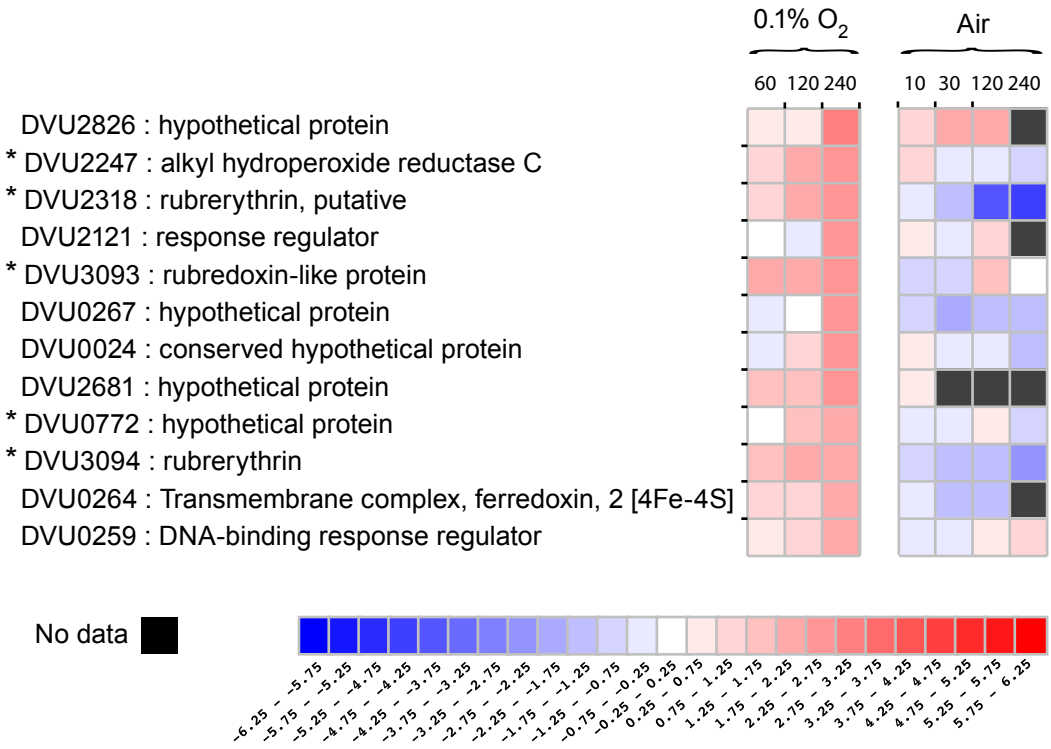
0.1% O2
Air
60 120 240
10 30 120 240
DVU2826 : hypothetical protein
* DVU2247 : alkyl hydroperoxide reductase C
* DVU2318 : rubrerythrin, putative
DVU2121 : response regulator
* DVU3093 : rubredoxin-like protein
DVU0267 : hypothetical protein
DVU0024 : conserved hypothetical protein
DVU2681 : hypothetical protein
* DVU0772 : hypothetical protein
* DVU3094 : rubrerythrin
DVU0264 : Transmembrane complex, ferredoxin, 2 [4Fe-4S]
DVU0259 : DNA-binding response regulator
No data
−6.25 − −5.75
−5.75 − −5.25
−5.25 − −4.75
−4.75 − −4.25
−4.25 − −3.75
−3.75 − −3.25
−3.25 − −2.75
−2.75 − −2.25
−2.25 − −1.75
−1.75 − −1.25
−1.25 − −0.75
−0.75 − −0.25
−0.25 − 0.25
0.25 − 0.75
0.75 − 1.25
1.25 − 1.75
1.75 − 2.25
2.25 − 2.75
2.75 − 3.25
3.25 − 3.75
3.75 − 4.25
4.25 − 4.75
4.75 − 5.25
5.25 − 5.75
5.75 − 6.25

DVU2410 : superoxide dismutase, Fe
DVUA0091 : catalase
DVU0019 : nigerythrin
DVU1984 : peptide methionine sulfoxide reductase MsrA
DVU1985 : conserved domain protein
DVU1228 : thiol peroxidase
DVU1839 : thioredoxin
DVU1838 : thioredoxin reductase
DVU1457 : thioredoxin reductase, putative
DVU0378 : thioredoxin, putative

DVU2483 : cytochrome c family protein
DVU0625 : cytochrome c nitrite reductase, catalytic subunit NrfA, putative
DVU2809 : cytochrome c3
DVU3271 : cytochrome d ubiquinol oxidase, subunit I
DVU3270 : cytochrome d ubiquinol oxidase, subunit II

DVU0536 : HmcA; high-molecular-weight cytochrome c
DVU0535 : 40.1 kd protein in hmc operon (HmcB)
DVU0534 : HmcC, 43.2 kd protein in hmc operon
DVU0533 : HmcD, 5.8 kd protein in hmc operon
DVU0532 : HmcE, 25.3 kd protein in hmc operon
DVU0531 : HmcF, 52.7 kd protein in hmc operon
DVU0530 : Rrf1 protein
DVU0529 : Rrf2 protein

DVU1770 : periplasmic [Fe] hydrogenase, small subunit
DVU2526 : periplasmic [NiFe] hydrogenase, large subunit, isozyme 2
DVU1918 : periplasmic [NiFeSe] hydrogenase, large subunit, selenocysteine-containing
DVU1917 : periplasmic [NiFeSe] hydrogenase, small subunit
DVU2287 : hydrogenase, CooK subunit, selenocysteine-containing, putative
DVU2286 : hydrogenase, CooM subunit, putative
DVU2290 : hydrogenase, CooU subunit, putative
DVU2289 : hydrogenase, CooX subunit, putative

DVU0774 : ATP synthase, F1 epsilon subunit
DVU0775 : ATP synthase, F1 beta subunit
DVU0776 : ATP synthase, F1 gamma subunit
DVU0777 : ATP synthase, F1 alpha subunit
DVU0778 : ATP synthase, F1 delta subunit
DVU0779 : ATP synthase F0, B subunit, putative
DVU0780 : ATP synthase F0, B subunit, putative

DVU3025 : pyruvate-ferredoxin oxidoreductase
DVU3026 : L-lactate permease family protein
DVU3027 : glycolate oxidase, subunit GlcD
DVU3028 : iron-sulfur cluster-binding protein
DVU3029 : phosphate acetyltransferase
DVU3030 : acetate kinase
DVU3024 : hypothetical protein

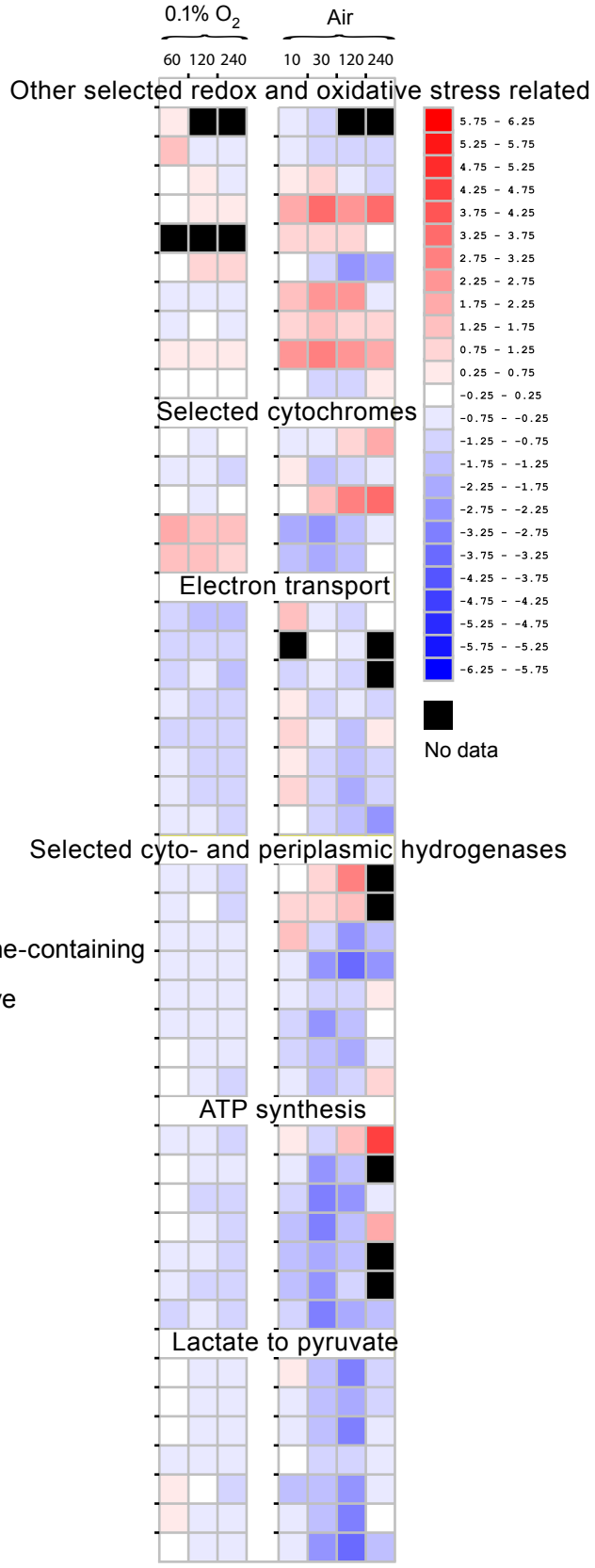

DVU3183 : desulfoferrodoxin
DVU3184 : rubredoxin
DVU3185 : rubredoxin-oxygen oxidoreductase
DVU0883 : glutaredoxin, putative
DVU0305 : ferredoxin II
DVU3276 : ferredoxin I
DVU1568 : ferritin

DVU0402 : dissimilatory sulfite reductase alpha subunit
DVU0403 : dissimilatory sulfite reductase beta subunit
DVU0846 : adenylylsulphate reductase, beta subunit
DVU0847 : adenylyl-sulphate reductase, alpha subunit
DVU0848 : Quinone-interacting membrane-bound oxidoreductase
DVU0849 : Quinone-interacting membrane-bound oxidoreductase
DVU0850 : Quinone-interacting membrane-bound oxidoreductase
DVU2776 : dissimilatory sulfite reductase, gamma subunit

DVU0105 : glutamine ABC transporter, ATP-binding protein
DVU0162 : carbamoyl-phosphate synthase, large subunit
DVU0386 : amino acid ABC transporter, periplasmic amino acid-binding protein
DVU0405 : cobyrinic acid a,c-diamide synthase
DVU0456 : DHH family protein
DVU1067 : membrane protein, Bmp family
DVU1069 : branched chain amino acid ABC transporter, permease protein
DVU1070 : branched chain amino acid ABC transporter, ATP-binding protein
DVU1286 : Integral membrane protein
DVU1287 : Periplasmic (Tat), binds 2[4Fe-4S]
DVU1288 : Periplasmic (Sec) triheme cytochrome c
DVU1289 : Cytoplasmic, binds 2 [4Fe-4S]
DVU1290 : Inner membrane protein binds 2 heme b
DVU1636 : inorganic pyrophosphatase, manganese-dependent
DVU1867 : diaminopimelate epimerase
DVU2108 : MTH1175-like domain family protein
DVU2310 : metallo-beta-lactamase family protein
DVU2735 : phenylacetate-coenzyme A ligase
DVU2825 : pyruvate formate-lyase 1 activating enzyme, putative
DVU3212 : pyridine nucleotide-disulfide oxidoreductase
DVU3290 : conserved domain protein
DVU3379 : ribonucleoside-diphosphate reductase
DVU0884 : conserved hypothetical protein
DVU0951 : molybdopterin biosynthesis MoeA protein, putative
ORF00713 : branched-chain amino acid ABC transporter, permease protein
DVU2103 : iron-sulfur cluster-binding/ATPase domain protein
DVU2271 : pyruvate formate-lyase activating enzyme, putative
ORF02867 : amino acid ABC transporter, ATP-binding protein
DVU2422 : nitroreductase family protein
DVU2990 : molybdopterin biosynthesis MoeA protein
DVU3113 : carbamoyl-phosphate synthase, small subunit

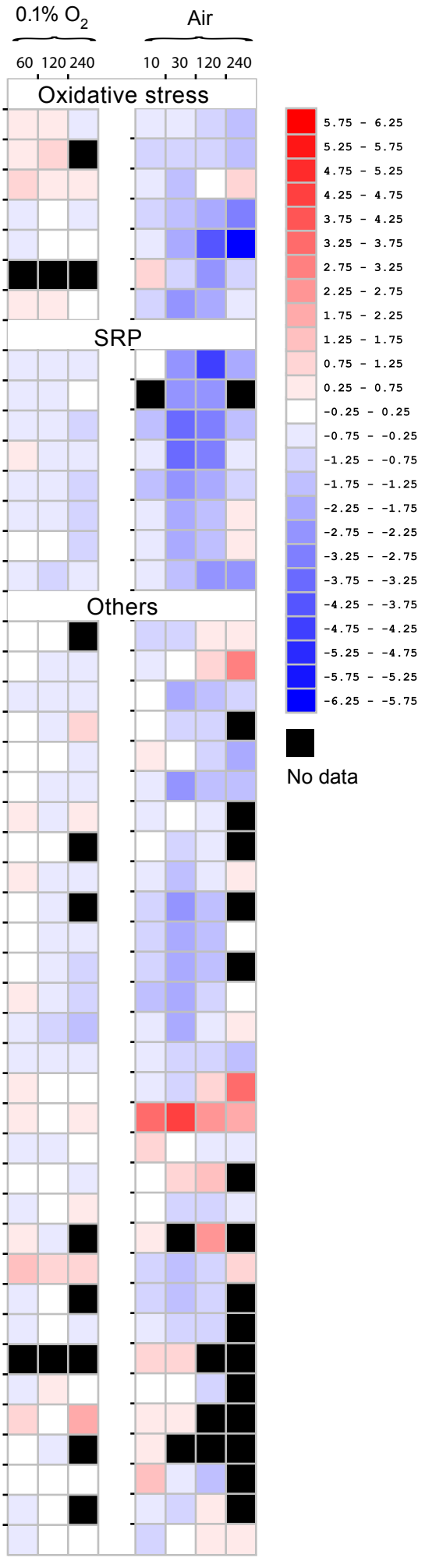

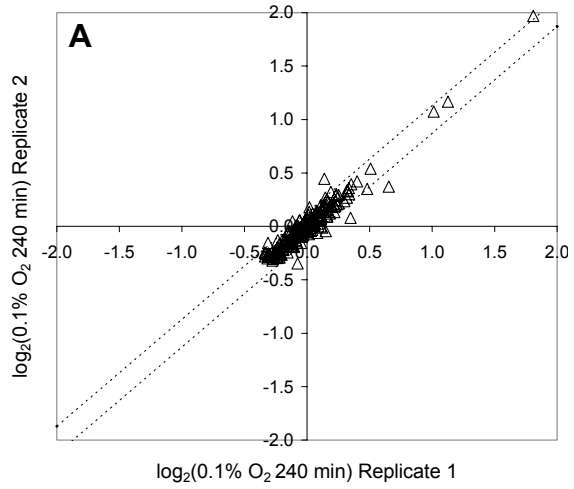
A
log2(0.1% O2 240 min) Replicate 2
log2(0.1% O2 240 min) Replicate 1

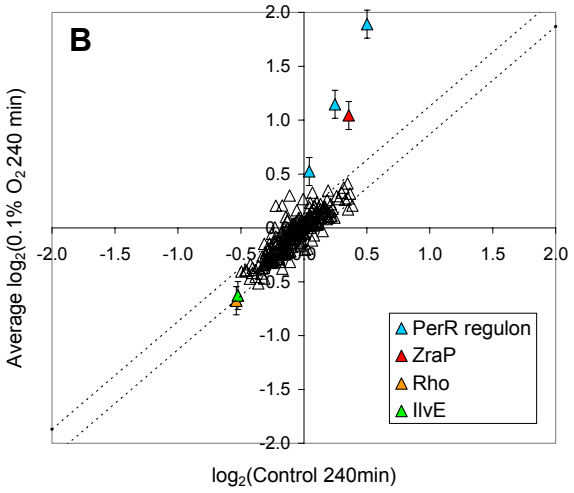
B
Average log2(0.1% O2 240 min)
log2(Control 240min)
PerR regulon
ZraP
Rho
IlvE

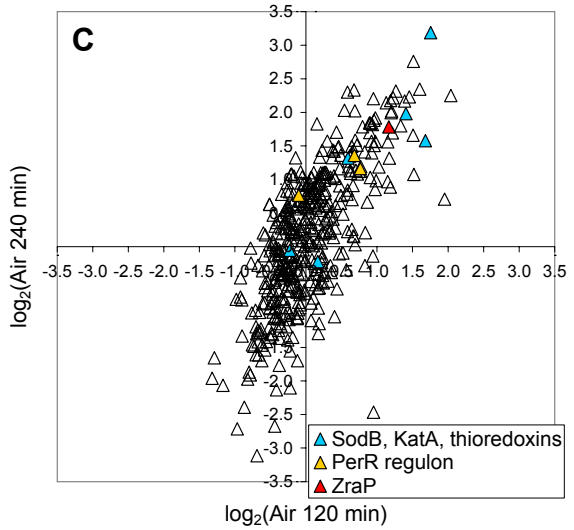
C
log2(Air 240 min)
log2(Air 120 min)
SodB, KatA, thioredoxins
PerR regulon
ZraP

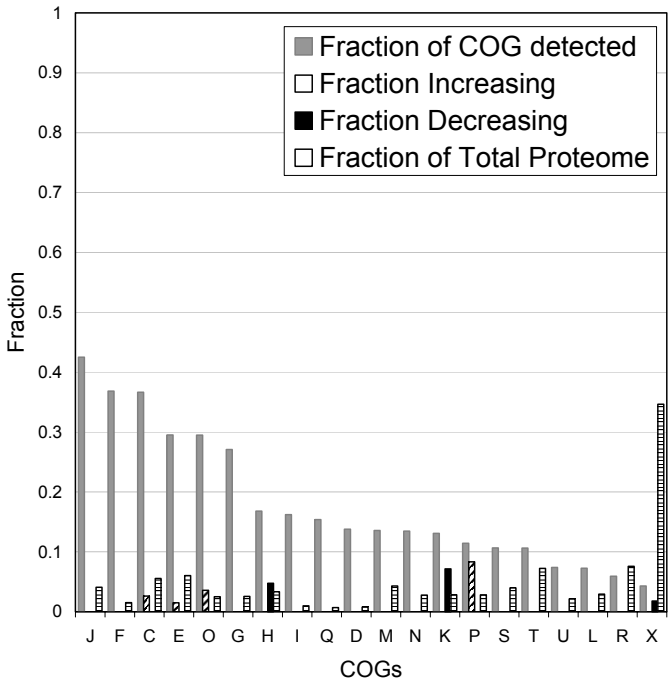

COG Category Description

B: Chromatin structure and dynamics
C: Energy production and conversion
D: Cell division and chromosome partitioning
E: Amino acid transport and metabolism
F: Nucleotide transport and metabolism
G: Carbohydrate transport and metabolism
H: Coenzyme metabolism
I: Lipid metabolism
J: Translation, ribosomal structure and biogenesis
K: Transcription
L: DNA replication, recombination, and repair
M: Cell envelope biogenesis, outer membrane
N: Cell motility and secretion
O: Posttranslational modification, protein turnover, chaperones
P: Inorganic ion transport and metabolism
Q: Secondary metabolites biosynthesis, transport, and catabolism
R: General function prediction only
S: Function unknown
T: Signal transduction mechanisms
U: Intracellular trafficking and secretion
V: Defense mechanisms
X: No annotated COG function

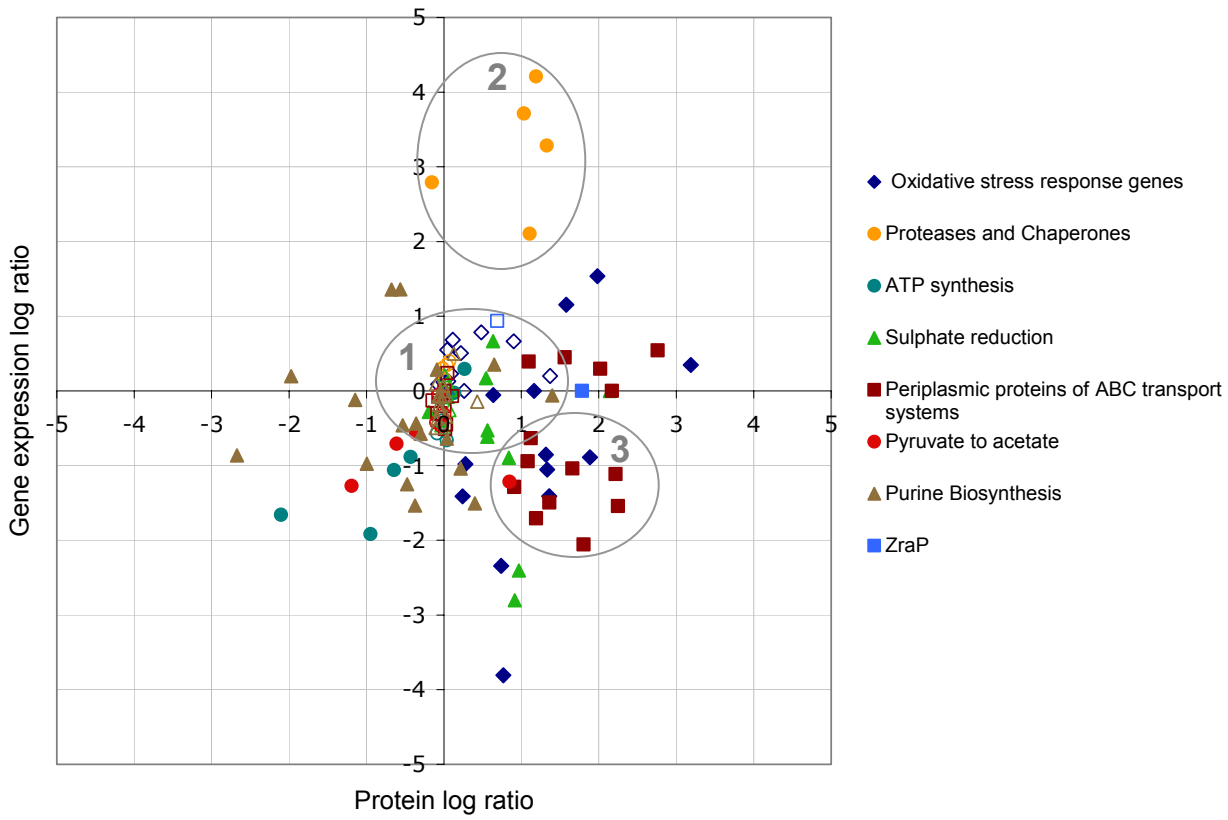
Gene expression log ratio
Protein log ratio
5
4
3
2
1
0
-1
-2
-3
-4
-5
-5
-4
-3
-2
-1
0
1
2
3
4
5
1
2
3
Oxidative stress response genes
Proteases and Chaperones
ATP synthesis
Sulphate reduction
Periplasmic proteins of ABC transport systems
Pyruvate to acetate
Purine Biosynthesis
ZraP

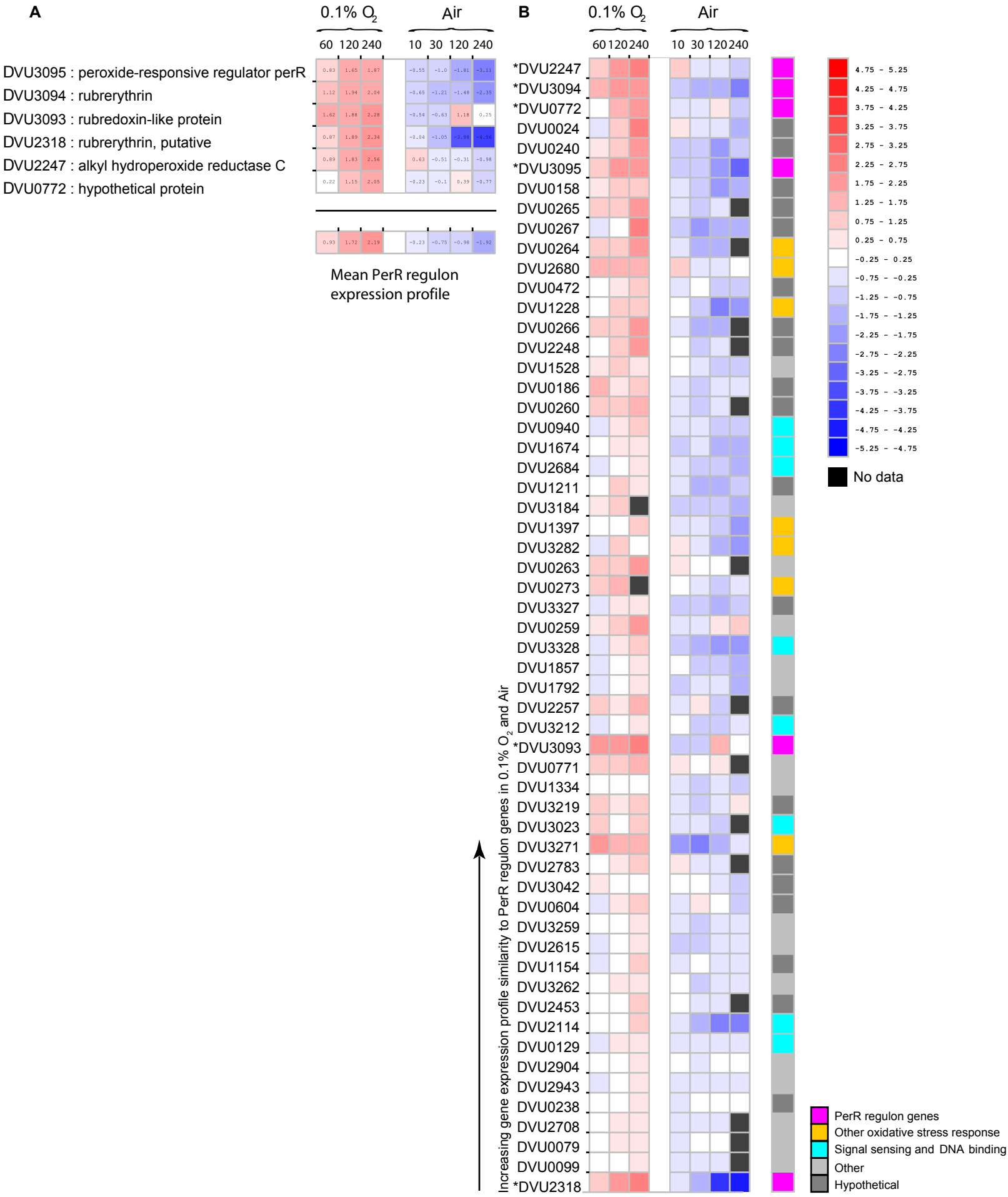
A
0.1% O2
Air
60 120 240
10 30 120 240
DVU3095 : peroxide-responsive regulator perR
DVU3094 : rubrerythrin
DVU3093 : rubredoxin-like protein
DVU2318 : rubrerythrin, putative
DVU2247 : alkyl hydroperoxide reductase C
DVU0772 : hypothetical protein
Mean PerR regulon expression profile
B
0.1% O2
Air
60 120 240
10 30 120 240
*DVU2247
*DVU3094
*DVU0772
DVU0024
DVU0240
*DVU3095
DVU0158
DVU0265
DVU0267
DVU0264
DVU2680
DVU0472
DVU1228
DVU0266
DVU2248
DVU1528
DVU0186
DVU0260
DVU0940
DVU1674
DVU2684
DVU1211
DVU3184
DVU1397
DVU3282
DVU0263
DVU0273
DVU3327
DVU0259
DVU3328
DVU1857
DVU1792
DVU2257
DVU3212
*DVU3093
DVU0771
DVU1334
DVU3219
DVU3023
DVU3271
DVU2783
DVU3042
DVU0604
DVU3259
DVU2615
DVU1154
DVU3262
DVU2453
DVU2114
DVU0129
DVU2904
DVU2943
DVU0238
DVU2708
DVU0079
DVU0099
*DVU2318
Increasing gene expression profile similarity to PerR regulon genes in 0.1% O2 and Air
4.75 - 5.25
4.25 - 4.75
3.75 - 4.25
3.25 - 3.75
2.75 - 3.25
2.25 - 2.75
1.75 - 2.25
1.25 - 1.75
0.75 - 1.25
0.25 - 0.75
-0.25 - 0.25
-0.75 - -0.25
-1.25 - -0.75
-1.75 - -1.25
-2.25 - -1.75
-2.75 - -2.25
-3.25 - -2.75
-3.75 - -3.25
-4.25 - -3.75
-4.75 - -4.25
-5.25 - -4.75
No data
PerR regulon genes
Other oxidative stress response
Signal sensing and DNA binding
Other
Hypothetical

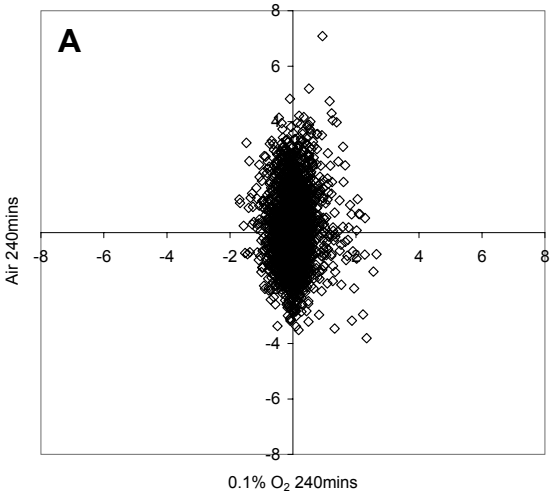
A
Air 240mins
0.1% O_2 240mins

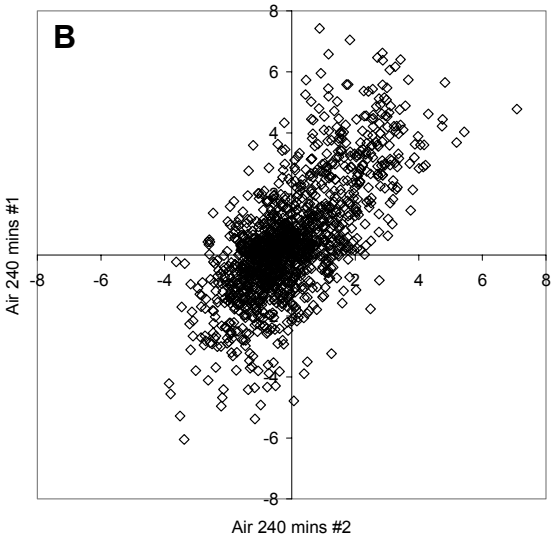
B
Air 240 mins #1
Air 240 mins #2

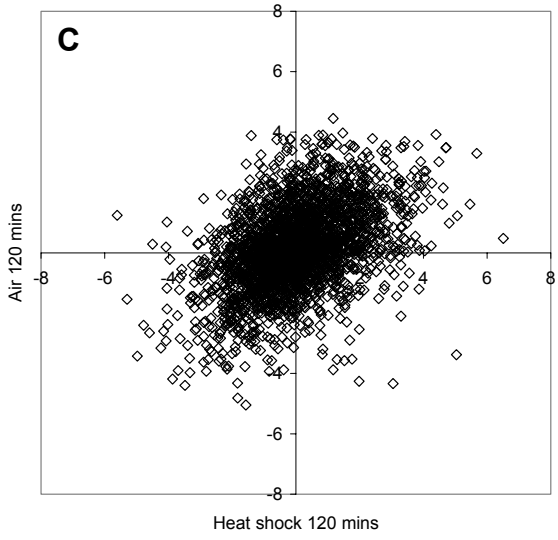
C
Air 120 mins
Heat shock 120 mins

Table 1. Selected Proteomics data.

DVU#	Gene name	Description	iTRAQ Log_2 (0.1% O_2 / control) 240mins (± 0.13) [a, b]	Microarray Log_2 (0.1% O_2 / control) 240mins [b]	iTRAQ Log_2 (Air / control) 240mins (± 0.13) [a, b]	Microarray Log_2 (air / control) 240mins [b]
Oxidative stress response proteins						
DVU0995	-	ThiJ/PfpI family protein	--	0.42 (0.8)	1.33 (1.16)	-1.05 (-1.89)
DVU1228	tpX	thiol peroxidase	0.16 (0.77)	0.5 (0.84)	0.24 (0.09)	-1.41 (-2.54)
DVU1397	bfr	bacterioferritin	-0.02 (0.05)	0.12 (0.22)	0.28 (0.13)	-0.98 (-1.18)
DVU1457	trxB	thioredoxin reductase, putative	0.15 (0.75)	0.11 (0.22)	1.98 (1.79)	1.53 (2.75)
DVU1568	ftn	ferritin	-0.13 (-0.38)	0.22 (0.38)	0.74 (0.58)	-2.34 (-4.3)
DVU1839	trx	thioredoxin	0.14 (0.7)	-0.1 (-0.18)	1.58 (1.4)	1.15 (1.84)
DVU2247	ahpC	alkyl hydroperoxide reductase C	1.89 (7.41)	0.19 (0.35)	1.36 (1.18)	-1.4 (0)
DVU2318	rbr2	rubrerythrin, putative	1.14 (4.56)	0.66 (1.13)	0.77 (0.6)	-3.8 (0)
DVU2410	sodB	superoxide dismutase, Fe	0.32 (1.4)	--	3.19 (2.97)	0.34 (0)
DVU3049	-	hemerythrin family protein	0.27 (1.19)	0.08 (0.14)	1.88 (1.7)	-0.89 (-1.41)
DVU3094	rbr	rubrerythrin	0.52 (2.16)	0.78 (1.36)	1.16 (0.99)	--
DVU3183	SOR	Superoxide reductase	--	0.59 (1.09)	1.69 (1.51)	2.31 (1.69)
DVU3185	roO	rubredoxin-oxygen oxidoreductase	0 (0.11)	0.54 (1.03)	0.64 (0.48)	-0.05 (-0.1)
DVUA0091	kat	Catalase	0.19 (0.9)	0.68 (0.84)	1.32 (1.14)	-0.85 (-1.25)
Proteases and Chaperons and other stress response						
DVU0811	dnaK	dnaK	0.03 (0.26)	0.24 (0.39)	1.03 (0.87)	3.28 (5.62)
DVU1012	-	hemolysin-type calcium-binding repeat	-0.39 (-1.37)	0.3 (0.45)	1.19 (1.02)	3.71 (0)
DVU1468	htrA	peptidase/PDZ domain	-0.36 (-1.27)	0.39 (0.74)	1.11 (0.94)	4.21 (6.74)
DVU1976	groEL	chaperonin, 60 kDa	-0.35 (-1.21)	0.34 (0.47)	-0.16 (-0.3)	2.1 (3.82)
DVU1977	groES	chaperonin, 10 kDa	--	0.15 (0.25)	1.33 (1.15)	2.79 (3.63)
DVU3384	zraP	zinc resistance-associated protein	1.04 (4.16)	0.93 (1.24)	1.78 (1.6)	--
Periplasmic proteins of ABC transport systems.						
DVU0095	potD-1	polyamine ABC transporter, periplasmic polyamine-binding	--	-0.5 (-0.84)	1.56 (1.38)	0.44 (0.81)
DVU0107	glnH	glutamine ABC transporter, periplasmic glutamine-binding	--	-0.1 (-0.19)	2.25 (2.05)	-1.54 (-2.74)
DVU0169	-	oligopeptide/dipeptide ABC transporter, periplasmic	0.09 (0.49)	-0.2 (-0.3)	2.22 (2.02)	-1.11 (-1.54)
DVU0386	glnH	amino acid ABC transporter, periplasmic	0.12 (0.62)	-0.44 (-0.77)	1.36 (1.18)	-1.49 (-2.82)
DVU0547	-	high-affinity branched chain amino acid ABC transporter, periplasmic	0.04 (0.3)	-0.29 (-0.51)	1.19 (1.02)	-1.7 (-3.33)
DVU0675	fliY	amino acid ABC transporter, periplasmic	0.22 (0.97)	--	2.17 (1.97)	--
DVU0712	-	amino acid ABC transporter, periplasmic-binding	0.25 (1.14)	-0.07 (-0.14)	1.08 (0.91)	-0.94 (0)
DVU0752	-	amino acid ABC transporter	-0.28 (-0.97)	-0.3 (-0.55)	1.1 (0.92)	0.39 (0.7)
DVU0966	-	amino acid ABC transporter, periplasmic	-0.14 (-0.41)	-0.5 (-0.92)	1.8 (1.62)	-2.05 (-3.6)
DVU1238	-	amino acid ABC transporter, periplasmic	--	-0.3 (-0.59)	1.66 (1.48)	-1.04 (-1.96)
DVU1937	-	phosphonate ABC transporter, periplasmic	-0.04 (-0.02)	-0.06 (-0.12)	0.91 (0.74)	-1.28 (-2.3)
DVU2297	-	glycine/betaine/L-proline ABC transporter, periplasmic-binding	0 (0.12)	0.23 (0.38)	2.02 (1.83)	0.29 (0.55)
DVU2342	-	amino acid ABC transporter, periplasmic	--	-0.51 (-0.93)	1.12 (0.95)	-0.63 (-1.03)
DVU3162	-	ABC transporter, periplasmic substrate-binding protein	0.09 (0.51)	-0.13 (-0.24)	2.76 (2.55)	0.54 (0)
ATP synthesis						
DVU0775	atpD	ATP synthase, F1 beta subunit	-0.21 (-0.68)	-0.39 (-0.63)	0.27 (0.11)	0.29 (0.35)
DVU0777	atpA	ATP synthase, F1 alpha subunit	-0.13 (-0.38)	-0.57 (-0.97)	0.13 (-0.01)	-0.02 (-0.02)
DVU0778	atpH	ATP synthase, F1 delta subunit	-0.24 (-0.78)	-0.66 (-0.94)	-0.43 (-0.57)	-0.88 (-1.42)
DVU0114	hisG	ATP phosphoribosyltransferase	--	-0.2 (-0.21)	-2.1 (-2.2)	-1.65 (-3.21)
DVU0779	atpF2	ATP synthase F0, B subunit	--	-0.89 (-1.56)	-0.64 (-0.78)	-1.06 (-1.17)
DVU0780	atpF1	ATP synthase F0, B subunit	--	-0.39 (-0.69)	-0.95 (-1.07)	-1.91 (-2.97)
Sulphate reduction						
DVU0402	dsrA	dissimilatory sulfite reductase alpha subunit	0.05 (0.35)	0.09 (0.17)	0.97 (0.8)	-2.4 (-2.49)
DVU0403	dvsB	dissimilatory sulfite reductase beta subunit	0.22 (1)	0.01 (0.01)	0.91 (0.75)	-2.8 (-4.74)
DVU0404	dsrD	dissimilatory sulfite reductase D	-0.02 (0.04)	0.2 (0.3)	2.14 (1.95)	--
DVU0847	apsA	adenylyl-sulphate reductase, alpha subunit	0.02 (0.25)	-0.08 (-0.13)	0.84 (0.67)	-0.89 (-1.32)
DVU0848	qmoA	Quinone-interacting membrane-bound oxidoreductase	-0.03 (0)	-0.5 (-0.89)	0.56 (0.4)	-0.61 (-1)
DVU0849	qmoB	Quinone-interacting membrane-bound oxidoreductase	-0.1 (-0.27)	-0.46 (-0.67)	0.54 (0.39)	0.16 (0.26)
DVU1295	sat	sulfate adenylyltransferase	0.07 (0.42)	-0.08 (-0.14)	-0.19 (-0.34)	-0.28 (0)
DVU1597	sir	sulfite reductase, assimilatory-type	-0.37 (-1.3)	-0.05 (-0.1)	0.63 (0.47)	0.66 (1.22)
DVU2776	dsrC	dissimilatory sulfite reductase, gamma subunit	-0.23 (-0.76)	-0.25 (-0.44)	0.56 (0.41)	-0.52 (-0.57)
Purine Biosynthesis						
DVU0161	purF	amidophosphoribosyltransferase	--	-0.22 (-0.37)	-0.36 (-0.5)	-0.43 (-0.72)
DVU0488	purD	phosphoribosylamine--glycine ligase	0.31 (1.37)	-0.06 (-0.08)	-0.56 (-0.7)	1.36 (0)
DVU0795	purC	phosphoribosylaminoimidazole-succinocarboxamide synthase	-0.02 (0.03)	-0.34 (-0.52)	-0.09 (-0.23)	0.28 (0.45)
DVU1043	guaA	GMP synthase	--	0.02 (0.03)	-0.68 (-0.81)	1.35 (2.62)
DVU1044	guaB	inosine-5`-monophosphate dehydrogenase	-0.21 (-0.7)	0.09 (0.15)	-1.15 (-1.26)	-0.12 (-0.21)
DVU1406	purM	phosphoribosylformylglycinamidine cyclo-ligase	--	-0.33 (-0.63)	-0.48 (-0.61)	-1.25 (-1.65)
DVU1932	adk	adenylate kinase (TIGR)	0.11 (0.57)	-0.49 (-0.68)	0.4 (0.24)	-1.5 (-2.97)
DVU2942	purB	adenylosuccinate lyase	0.2 (0.93)	-0.14 (-0.24)	0.65 (0.49)	0.35 (0.53)
DVU3181	purL	phosphoribosylformylglycinamidine synthase II	0.04 (0.32)	-0.18 (-0.28)	-1.97 (-2.07)	0.19 (0.34)
DVU3204	purA	adenylosuccinate synthetase	0 (0.11)	--	0.04 (-0.11)	-0.64 (-1.16)
DVU3206	purH	phosphoribosylaminoimidazolecarboxamide formyltransferase	--	0.28 (0.5)	-0.37 (-0.51)	-1.53 (-3.02)
DVU3235	purH	IMP cyclohydrolase, putative	0.26 (1.17)	0.06 (0.11)	1.4 (1.22)	-0.06 (-0.11)
Pyruvate to acetate						
DVU3025	por	pyruvate-ferredoxin oxidoreductase	-0.3 (-1.03)	-0.04 (-0.07)	-0.36 (-0.5)	-0.56 (-0.8)
DVU3027	glcD	glycolate oxidase, subunit	-0.23 (-0.75)	-0.42 (-0.77)	-0.61 (-0.74)	-0.7 (-0.81)
DVU3029	pta	phosphate acetyltransferase	-0.29 (-1)	-0.47 (-0.81)	-1.19 (-1.31)	-1.27 (0)
DVU3030	ackA	acetate kinase	0 (0.16)	-0.31 (-0.54)	0.85 (0.68)	-1.21 (-1.36)

[a] ± 0.13 represents the internal error cut-off as computed in the methods section

[b] Values shown are log_2 ratios, in paranthesis are the corresponding z-scores; only values for which z-score is≥ 2 were considered significant change